Material Compatibility for Passive Two-Phase Immersion Cooling Applications

by

Alexander Lee Kelly

A thesis submitted to the Graduate Faculty of
Auburn University
in partial fulfillment of the
requirements for the Degree of
Master of Science

Auburn, Alabama
May 3, 2014

Keywords: Dielectric Fluids, Characterization, Thermal Management

Approved by

Virginia A. Davis, Chair, Sanders Associate Professor of Chemical Engineering
Steve R. Duke, Alumni Associate Professor, Samuel Ginn College of Engineering
Allan E. David, John W. Brown Assistant Professor of Chemical Engineering
Michael C. Hamilton, Assistant Professor of Electrical and Computer Engineering

Abstract

The objective of this work was to investigate potential material compatibility issues related to immersion cooling for high performance computing applications. Extended exposure of potential performance computing components and fluid handling materials to 3M's Novec™ 649, Novec™ HFE-7100, and Fluorinert™ FC-72 engineered fluids was simulated using a Soxhlet extractor. This accelerated testing led to chemical elution from some polymeric materials into the fluid. In most cases, the fluid contaminants were polymer additives, particularly plasticizers. The contaminants were identified using attenuated total reflectance Fourier transform infrared (ATR-FTIR) spectroscopy as well as gas chromatography/mass spectrometry (GC/MS). The total contaminant concentrations were determined using mass balances. In addition, an ultraviolet-visible spectroscopy (UV-Vis) calibration curve was developed to measure the concentration of dioctyl phthalate (DOP) extracted from poly(vinyl chloride) (PVC) into the fluids. UV-Vis was also used to show the amount of DOP that could be removed from the fluid using consumer grade activated carbon. The use of fundamental thermodynamic relationships for selection of compatible materials with dielectric fluids was also explored. Additional thermodynamic modeling research would enable formulation and/or selection of materials with improved compatibility. Meanwhile, the empirical data has resulted in material selection guidelines for passive two-phase immersion cooling using the engineered dielectric fluids.

Acknowledgements

I would like to thank Dr. Virginia A. Davis for her support and guidance throughout the course of this work and my graduate studies. I would like to thank my committee members for their knowledge and time in the critical review and preparation of this manuscript. I would also like to thank Alexander Haywood, Joyanta Goswami, and Teng (Daisy) Xu for their assistance with many aspects of this work.

Personal gratitude is also extended to Dr. Mario Eden and Dr. Robert Ashurst for their guidance unrelated to research.

Finally, this work would not have been possible without the continued support from Mary Ann and Thomas J. Kelly.

Table of Contents

List of Figures

List of Tables

Chapter 1

Introduction

To date, a scientific approach to analyzing the interaction between immersion cooling fluids and computing materials has not been developed. This thesis presents a detailed investigation of material compatibility for use within passive two-phase immersion cooling applications. Accelerated testing using a Soxhlet extraction technique allowed for the characterization of the effects of prolonged exposure of dielectric fluids to component materials. Leaching of solid materials and additives such as plasticizers was discovered via optical microscopy as well as infrared and ultraviolet spectroscopy techniques. The concentrations of extractable components were quantified to the extent possible. Preliminary investigation of changes in the physical properties of polymeric materials was conducted. In addition, a potential remediation method for organic contaminants was proposed via the use of activated carbon adsorption. A database of infrared spectroscopy spectra was developed and unknown material extracts from application testing were matched to leached components from broad spectrum analysis of potential computing materials. Design considerations and guidelines were proposed for passive two-phase immersion cooling implementation within commercial applications.

The removal of heat from power electronics and performance computing systems is a growing problem. The increase in component speed and circuitry density results in an increased heat flux at the chip and package level. Removal of this additional heat has

garnered interest into advanced cooling techniques. Recent research has documented the efficiency and performance potential immersion cooling has over other, more complex systems. Although the benefits of immersion cooling have been well demonstrated, component compatibility and material design considerations have not been examined in detail. There is a need for large scale investigation of potential compatible materials and resulting long term exposure to cooling fluids. Knowledge of and remediation techniques for the removal of extractable components from long term exposure to immersion cooling fluids are vital design considerations in moving forward with the development and application of immersion cooling systems.

Figure 1 provides a graphical outline of this research. The document is organized in the following manner: Chapter 2 provides a background of the materials and techniques used throughout the course of this work. Chapter 3 is a description of the experimental work performed including general operating principles for the instrumentation. Chapter 4 describes the experimental results. Chapter 5 concludes the document and provides suggested design considerations for implementation of immersion cooling within high performance computing (HPC) applications.

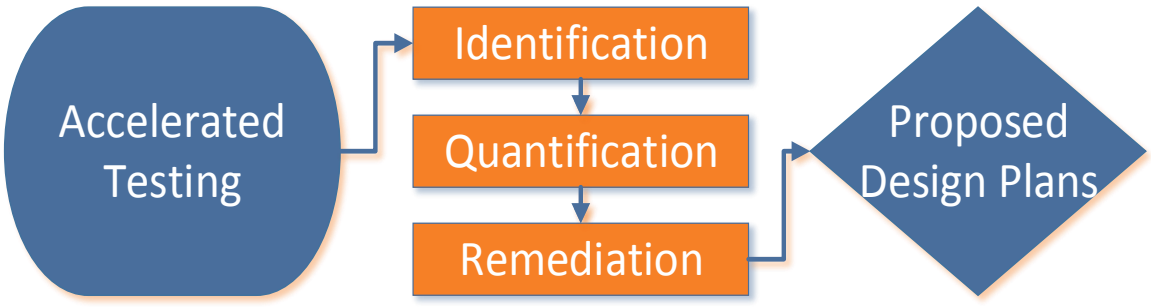

Figure 1. Accelerated testing and analysis overview.

Chapter 2

Background

2.1 Thermal Management

The rapid development of modern computing technology has led to an increase in the packing density of integrated circuits. This in turn has led to the production of high power density microelectronic devices. With an increased density has come increases in heat production at the chip and package level. In addition, high performance computing system designers struggle with the limitation of increased heat production. Increases in temperature affect the performance and reliability of integrated circuits when working outside of the desired operating range. The control and removal of heat is of particular importance and has led to significant research efforts in developing novel techniques and refining the use of traditional cooling methods.

The flow of heat within a process is a function of the heat transfer coefficient, heat transfer surface area, and the temperature difference. An increase in heat removal within a system is achieved by increasing either of these variables. Increasing the temperature difference is often limited by the process or material constraints; maximizing the surface area of heat transfer is a common macro-scale technique that cannot be applied to the growing microelectronics industry. Thus, manipulation of the heat transfer coefficient has become of particular interest [1].

The heat transfer coefficient is often increased by improving the heat transfer method or transport properties of the material itself. Traditional cooling techniques such as air cooling have often been combined with heat sinks to make use of forced convection. However, air cooling is not effective within applications that maintain heat fluxes greater than 100 W/cm^2 or systems that do not lend themselves to the physical dimensions necessary for proper implementation. Microchannel heat sinks have been combined with the superior thermal properties of liquid cooling for increased cooling capability through single-phase forced convection [2]. Recently, there has been investigation on the addition of colloidal and nano-sized particles within heat transfer fluids for increased thermal performance. However, much of this research remains plagued with inconsistent results due to a lack of dispersion characterization and method description [3].

Immersion of electronic components within inert liquid for cooling has been practiced in a number of areas of microelectronics. Immersion cooling has significant advantages over air cooling in that the heat transfer rate is increased and the liquid has a higher heat capacity than that of a gas. In addition, engineered dielectric thermal fluids, such as fluoroether and fluoroketone liquids from 3M, have advantageous physical properties such as low boiling points and large fluid temperature ranges [4-6]. The lower boiling points allow the implementation of two-phase cooling in which the fluid in direct contact with the integrated circuits undergoes a phase change from liquid to vapor. This particular method of cooling uses the latent heat of the fluid rather than its sensible heat. This allows the coolant and heat sink to remain at constant temperatures.

Passive two-phase immersion cooling can be simpler and less costly than single-phase forced convection cooling methods since equipment costs such as fans, heat sinks,

pumps, and hoses are no longer needed. In addition, the thermal performance is often superior [7]. Although immersion cooling has several significant advantages over traditional cooling methods, it is not without shortcomings. The heat transfer characteristics between the fluid and integrated circuits are not yet well understood. In addition, the material compatibility between the engineered fluids and the component materials found within computing systems remains to be characterized. Further advances in mechanical and electrical construction of the electronic assembly remain to be completed to take full advantage of the capabilities of immersion cooling [8].

2.2 Dielectric Fluids

Dielectric strength is a measure of a material's electrical stability as an insulator. The maximum voltage required to produce a dielectric breakdown is termed the dielectric strength and is expressed in volts per unit thickness. A higher dielectric strength correlates to a higher quality insulator. Dielectric strength is affected by the operating temperature and frequency of electric field. The dielectric strength of a material is often measured by one of three procedures: short-time method, slow-rate-of-rise method, and step-by-step method. All three methods entail placing a sample of material between two electrodes and ramping the voltage at a consistent rate until dielectric breakdown is determined [9].

Dielectric fluids are used as electrical insulators in a variety of high voltage applications including transformers, high voltage cabling, and microelectronic systems. Ideal dielectric fluids have a high dielectric strength, thermal stability, and chemical inertness while also being non-flammable, non-toxic, and environmentally friendly. In addition, dielectric fluids are often used as a method for heat dissipation. Traditional

dielectric fluids include mineral oil, silicone oil, and purified water with each possessing key characteristics ideal for use in specific applications [10]. Engineered fluids represent an attempt by companies such as 3M to develop dielectric fluids that have a broader range of applications by possessing higher heat capacities, greater chemical inertness, and wider operating conditions, all while yielding a decreased environmental impact.

3M Novec Engineered fluids and 3M Fluorinert Electronic liquids are a class of thermal management fluids with boiling points ranging from 34°C to 175°C and freezing points from -38°C to -138°C. Figure 2 shows the chemical structures of the three fluids investigated. Novec 649 has the lowest global warming potential within the Novec family. Novec 7100, commonly referred to as HFE-7100, is a mixture of n- and iso-butyl isomers of methoxyperfluorobutane. FC-72 is a member of the Fluorinert family and is fully fluorinated (perfluorohexane). This perfluorinated structure provides significant chemical inertness. Novec 649's fluoroketone structure suggests that it has an intermediate solvent power, whereas HFE-7100's ether linkage and hydrogenated portion increase its solvent power over the other two fluids. Novec 649 was chosen as the most applicable fluid for testing given its thermal properties.

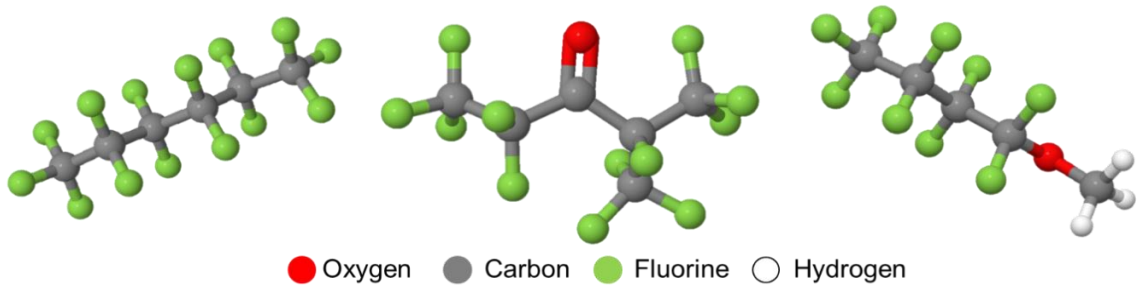

Figure 2. Chemical structure of FC-72 (left), Novec 649 (center), and HFE-7100 (right).

Table 1 provides some of the physical and thermal properties of the engineered fluids chosen for testing. It should be noted that the dielectric properties of Novec 649 ($C_6F_{12}O$) are similar to those of FC-72 (C_6F_{14}). HFE-7100 ($C_5F_9OH_3$) has a significantly higher dielectric constant and lower resistivity. Novec 649's global warming potential of 1 is among the lowest of any man-made compound. These specific thermal properties make all these fluids well suited for heat transfer systems, but Novec 649 was the primary focus of this research due to its preferential combination of thermal and dielectric properties.

Table 1. Physical properties of engineered fluids used for immersion cooling [5, 11].

Property	Working Fluid		
Trade Name	FC-72	HFE-7100	Novec 649
Molecular Formula	C_6F_{14}	$C_5F_9OH_3$	$C_6F_{12}O$
Fluid Type	PFC	HFE	FK
T_b [°C]	56	61	49
$T_{critical}$ [°C]	178	195	169
$P_{critical}$ [MPa]	1.83	2.23	1.88
T_{freeze} [°C]	<-100	<-100	<-100
T_{flash} [°C]	None	None	None
σ [mN/m]	12.0	13.6	10.8
k [W/m-K]	0.057	0.069	0.059
Cp of liquid [J/kg-K]	1050	1183	1103
ρ [kg/m^3]	1680	1510	1600
ν [cSt]	0.40	0.38	0.40
h @ T_b [kJ/kg]	88	112	88
P_{sat} at 25 °C [kPa]	30.9	27	40.4
Resistivity [Gohm-cm]	1000000	0.1	10000
Dielect. Const.	1.76	7.4	1.84
DS [kV@2.54 mm]	~40	~40	~40
GWP	9300	297	1
EG [ppmv]	NA	750	150

2.3 Accelerated Testing

Accelerated testing took place primarily within a Soxhlet extraction apparatus. Soxhlet extraction is a standard chemistry method used to extract nonvolatile and semivolatile organic compounds from a solid sample that typically have a low solubility in the solvent. This type of extraction is commonly referred to as solid-liquid extraction. As depicted in Figure 3, a solid sample material (1) is placed within the thimble holder. During operation, this thimble is gradually filled with newly condensed solvent from the distillation flask. Solvent boils within the distillation flask (3) producing a vapor that travels up the vapor tube (6) to the condenser (7). The condensed solvent then falls into the thimble holder (8). When the solvent level reaches the overflow level (9), the siphon aspirates the fluid within the thimble holder back into the distillation flask (10), taking with it any extracted analytes. The solvent is then recirculated though the system and the process continues [12].

Soxhlet extraction provides many advantages over other extraction methods such as supercritical fluids. These advantages include simplicity, relatively high system temperatures, and a constant concentration gradient. A high system temperature is observed as the heat from the boiling solvent within the distillation flask reaches the extraction cavity. Since the fluid in contact with the component material is distilled, the analyte concentration within the solvent is effectively zero. This continual reintroduction of fresh solvent prevents the chance of a reduction in the concentration gradient driving force for extraction. In addition, increased sample throughput or breadth can be achieved by running simultaneous extractions [7, 12].

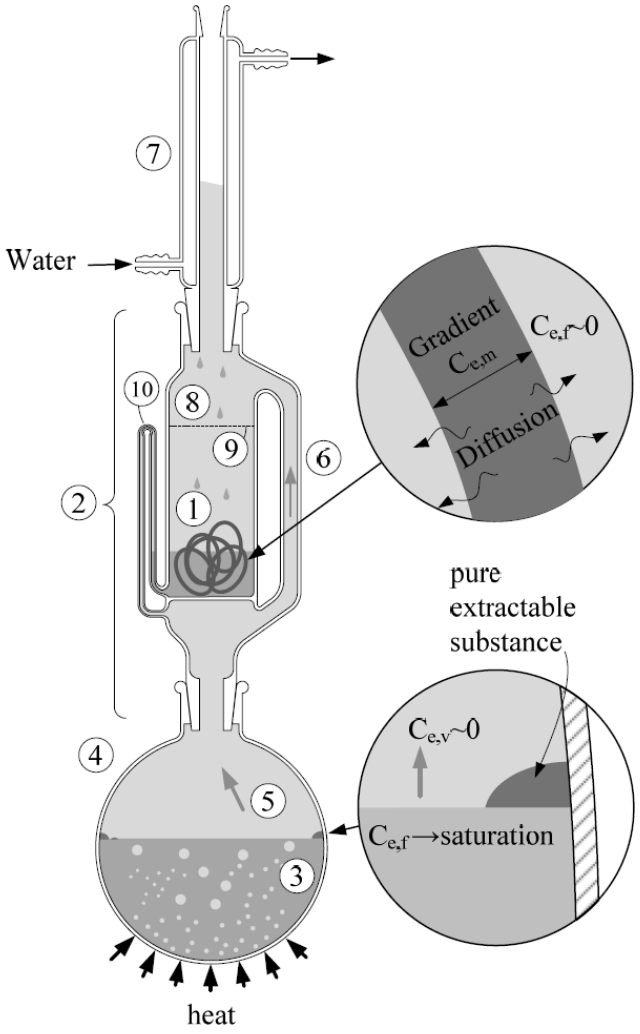

Figure 3. Soxhlet extraction apparatus and key extraction parameters [7].

Some of the drawbacks of Soxhlet extraction include the long time necessary for extraction compared to other techniques. Although 3M states that forty-eight hours is sufficient to remove most of the substance from a 1mm thick elastomer sample, longer extraction periods were needed for large component materials [7]. In addition, the large amount of solvent required for proper operation of the Soxhlet apparatus represents a significant cost of operation. Due to the increased temperature necessary to boil the solvent, thermal decomposition of samples is a possibility where solvent boiling points are

high. In addition, the direct contact the component material has with the solvent potentially leaves the component with absorbed and/or adsorbed fluid which may affect subsequent analysis. Soxhlet extraction was chosen over other extraction techniques for its similarity with the process predicted within immersion cooling applications. While more advanced extraction techniques such as microwave or ultrasound assisted Soxhlet extraction would have potentially yielded a greater analyte concentration, the processes were less indicative of the immersion cooling applications.

In a limited case, passive hexane extraction of polymeric materials was conducted. Passive extraction was utilized over hexane within the Soxhlet apparatus for safety concerns. Provided that hexane is a much stronger solvent than the dielectric fluids under consideration, it was used to extract large amounts of plasticizer from polymeric materials (e.g., poly vinyl choloride). HallStar indicates that 85% of the contained plasticizer content within PVC can be extracted via soaking in hexane [13].

2.4 Computing Materials

High performance computing and high heat flux computing systems are constructed of numerous types of materials. In passive two-phase immersion cooling, the fluid is in direct contact with computing system materials. Although most of the performance centered materials are constructed of metals and metalloids, a significant portion of the remaining components are made of, or coated with, polymeric materials. These components include casings, fixtures, interconnects, and packaging. Thus, it is necessary to consider the chemical makeup of these materials, specifically polymeric materials. A list of materials chosen for analysis is provided in Appendix A – Materials Included in

Screening Study. These materials included those that may be used in application, test tanks, or are typically used in laboratory or commercial handling and sealing of fluids. It was understood that not all of the materials named would be used in high performance computing applications, but a comprehensive approach was taken to evaluate all potentially viable materials.

The primary concern in immersion cooling is the leaching of polymer additives into the dielectric fluids. Many polymeric materials contain additives to tailor properties including stability, flexibility, color, and surface chemistry. Typically, multiple additives are needed to obtain the desired properties for a given application. For example, poly(vinyl chloride) (PVC) typically includes additives such as antioxidants, blowing agents, flame retardants, impact modifiers, plasticizer, and a UV stabilizer [14, 15]. The world additives market amounts to 7.8 million tonnes and is projected to grow 3.5-4 % per year [16].

Plasticizers are of particular interest in that they are usually included in order to produce flexible plastics for specific applications. Plasticizers are also used to lower a polymer's melt viscosity to facilitate processing. Flexible plastics are achieved by the inclusion of a plasticizing agent. This plasticizing agent acts as a lubricant between polymer molecules and increases its free volume. There are two distinct classes of plasticizers, those that are dissolved in the polymer (external) and those that are chemically bonded to the polymer (internal). Through reaction, internal plasticizers lead to a reduction in the molecular weight of the polymer [17]. Table 2 provides a list of commonly used external plasticizers and their abbreviations.

Table 2. Commonly used external plasticizers and abbreviations [14, 18].

Plasticizer	**Abbreviation**
Aromatic esters	
Dibutyl phthalate	DBP
Dimethoxyethyl phthalate	
Di-2-ethylhexyl phthalate	DOP, DEHP
Di-*n*-undecyl phthalate	
Di-*n*-tridecyl phthalate	
Butyl benzyl phthalate	
Butyl octyl phthalate	
Tri-2-ethylhexyl trimellitate	
Aliphatic esters	
Di-2-ethylhexyl adipate (DOA)	DOA
Di-*n*-butyl sebacate (DBS)	DBS
Di-2-ethylhexyl sebacate (DOS)	DOS
Di-2-ethylhexyl azelate	DIDA
Epoxidized oils	
Epoxidized soybean oil	
Epoxidized linseed oil	
Epoxidized tall oil fatty adds	
Flame retardant	
Aryl and atylalkyl phosphates	
Chlorinated paraffins	
Polymeric	
Poly(alky1ene adipates, sebacates, and azelates	
Acrylonitrile-butadiene copolymers	

Phthalates account for 92% of the plasticizers produced worldwide with DOP representing 51% [17]. DOP has been used extensively since its introduction in 1930. Phthalate esters were initially determined to be benign to humans [19]. This led to their use within medical plastics and children's toys. More recent research has brought phthalate esters' biocompatibility into question upon evidence of migration. Phthalates are often used in polymeric materials that are in intimate contact with medical solutions. Issues such as migration and leaching are of particular concern during storage [20]. Shah et al. demonstrated the loss of plasticizer from PVC over a seven day period from migration to

silica gel. A total of 40% plasticizer was used with various blends of DOP, butyl benzyl phthalate (BBP), isodecyl diphenyl phosphate (IDDP), and polybutylene adipate (PBA). Figure 4 shows that the replacement of DOP with other plasticizers leads to decreased migration from PVC. The migration of plasticizer within the PVC sample was deemed to be a function of the molecular weight of the species [20].

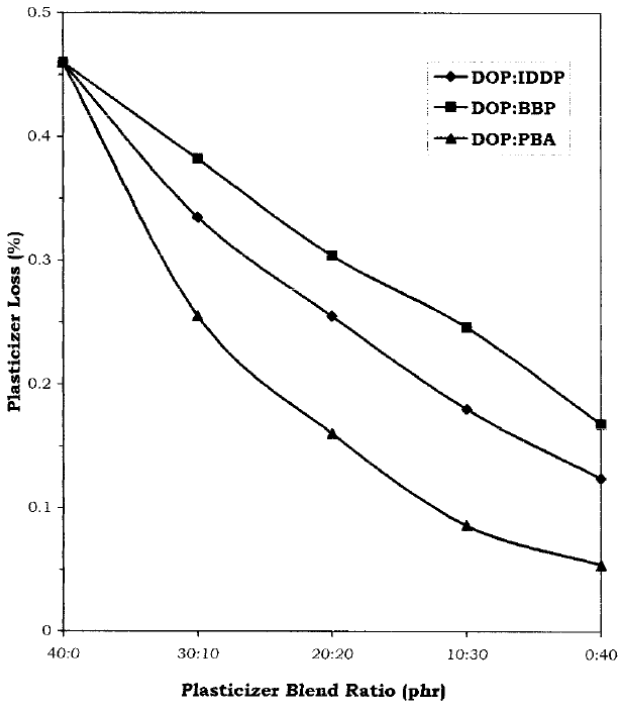

Figure 4. DOP migration from PVC over seven day period of exposure to silica gel [20].

In the same study, Shah et al. demonstrated that the dielectric strength of PVC increases with decreasing DOP concentration following ASTM D-149. Figure 5 shows that as the ratio of the other included plasticizers increases so does the dielectric strength. Migration, specifically liquid leaching, is of most concern for high performance computing systems in which polymeric materials make up a large subset of components. The effect

of increased plasticizer concentration within dielectric fluids is of particular concern. Such issues need to be accounted for within application implementation of passive two-phase immersion cooling. Table 3 provides a list of plasticizer-related technical challenges.

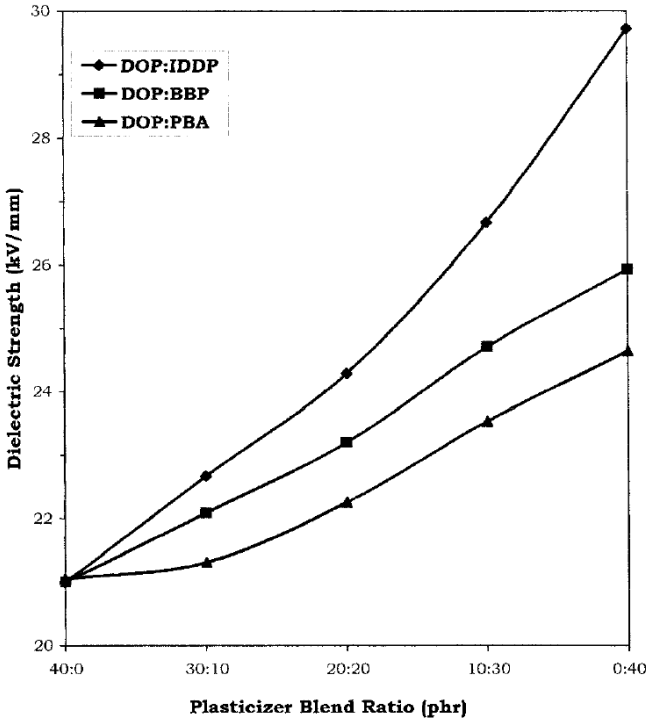

Figure 5. Changes in dielectric strength as the concentration of DOP present within PVC decreases [20].

Table 3. Plasticizer-related technical challenges [17].

Migration out of plastic
Solid–solid migration
Evaporation
Liquid leaching
High temperature flexibility
Low temperature lubricity
Health and environmental effects (cytotoxicity)
Flammability concern regarding plasticizers
Compatibility with new polymers
Stability to ultraviolet rays
Biodegradability
Improved material lifetime

2.5 Solubility Parameters

The migration of plasticizers within immersion cooling applications is a function of the polymer, plasticizer, and dielectric fluid. The movement of plasticizer though the polymer (permeation) depends on the solubility and diffusion coefficients of the plasticizer in the polymeric material [21]. Diffusion of some plasticizers within PVC is described by Fick's second law, where the diffusion coefficient is a function of the concentration gradient, and is impacted by the morphology of the polymer [22, 23]. Solubility, as it relates to plasticizers and dielectric fluids, is the capacity of the fluid to uptake plasticizer. Extending these relationships to immersion cooling applications may provide the use of solubility parameters in predicting the interaction of component materials and dielectric fluids.

The term solubility parameter refers to the value of a quantity δ that is often used in a semi-quantitative manner to predict and interpret the thermodynamic likeness of two components. There are many parameters in use today including the Kauri-Butanol number, heptane number, analine cloud point, Hildebrand solubility parameter, and the Hansen Solubility parameter. All of the parameters are relative to their particular scale and typically can be converted between systems except for those that are based purely on empirical relationships. Interestingly, Tuma et al. used the KB value to describe engineered fluids even though this parameter was empirically developed for a dramatically different class of chemicals [7].

2.5.1 Kauri-Butanol

Kauri-Butanol (KB) has been used to measure engineered fluid solvent power based upon ASTM standard D1133 for hydrocarbon solvents. However, it is typically used to describe solvents within paint and lacquer formulations with an initial boiling point over 40°C and a dry point under 300°C. The KB value of solvents is the volume of solvent necessary to produce a defined degree of turbidity when added to 20 g of a standard solution of kauri resin in n-butyl alcohol. A higher KB value indicates a stronger solvency. In a typical experiment, a solvent of interest is titrated into a solution of kauri resin located within an Erlenmeyer flask. The endpoint of this titration is determined when the sharp outlines of 10-point print placed directly under the Erlenmeyer flask is blurred or obscured. The volume of solvent, in mL, needed to reach the endpoint of titration *C* is inserted into Equation 2.1 along with the volume of toluene *A* and a heptane-toluene blend consisting of 25 ± 0.1% toluene and 75 ± 0.1% n-heptane *B* required to titrate the same solution, in mL [24].

Table *4* provides the KB values of the three dielectric fluids used in this work.

$$KB = \frac{65(C-B)}{(A-B)} + 40 \tag{2.1}$$

Table 4. 3M dielectric fluid KB values [7].

Dielectric Fluid	KB Value
Novec 649	0
HFE-7100	10
FC-72	0

2.5.2 Hildebrand Solubility Parameter

Joel H. Hildebrand laid the foundation of modern solubility theory when he proposed that the square root of the cohesive energy density yielded a value representative of a solvent's relative solvency power. The Hildebrand parameter is a numerical estimation of the attractive forces between molecules better known as the van der Waals forces. These forces can be split into three categories: London dispersion forces, dipole induced-dipole interactions (Debye), and permanent dipole-dipole interactions (Keesom). Given its foundation, the Hildebrand parameter is most applicable to non-polar solvents. In addition, the solubility parameter of solvent mixtures can be calculated by averaging the Hildebrand values of the individual solvent components [25].

A working definition of the Hildebrand solubility parameter δ is often used

$$\delta = \left(\frac{-E}{V^l}\right)^{0.5} \tag{2.2}$$

where $-E$ is the energy of vaporization to the gas phase with infinite separation of the molecules and V^l the molar volume of the liquid [26]. At low vapor pressures, the vapor-liquid equilibrium is considered ideal and allows for the simplification of Equation 2.2 to Equation 2.3

$$\delta = \left(\frac{\Delta \mathrm{H}^V - RT}{V^l}\right)^{0.5} \tag{2.3}$$

where $\Delta \mathrm{H}^V$ is the heat of vaporization, R the ideal gas constant, and T is the temperature. This simplification directly allows the calculation of the Hildebrand parameter calorimetrically. For polymeric materials, swelling behavior is often used to assign Hildebrand values [26]. The units of the Hildebrand parameter are often expressed as $\mathrm{MPa}^{0.5}$, which is 2.0455 times larger than that in $\mathrm{cal}^{0.5}\mathrm{cm}^{-1.5}$.

2.5.3 Hansen Solubility Parameter

The Hansen solubility parameter (HSP) is closely related to the Hildebrand parameter in that it attempts to further delineate the interactions between molecules. Hansen describes the total energy of vaporization of a liquid as consisting of (atomic) dispersion forces, (molecular) permanent dipole-permanent dipole forces, and (molecular) hydrogen bonding. Hansen attempts to provide potentially more information regarding solubility by breaking down the fundamental interactions into three components, shown in Equation 2.4, where the total cohesive energy, *E*, is the sum of the energies that encompass it

$$E = E_D + E_P + E_H \tag{2.4}$$

where E_D is the energy from dispersion forces, E_P the polar cohesive energy, and E_H the electron exchange parameter. Dividing Equation 2.4 by the molar volume gives the square of the total (Hildebrand) solubility parameter as the sum of the squares of the individual Hansen components (Equation 2.5) in $MPa^{0.5}$

$$\delta^2 = \delta_D^2 + \delta_P^2 + \delta_H^2 \tag{2.5}$$

The HSP can potentially allow for more accurate determination of solvent interactions since component parameters can now be compared. For example, nitromethane and ethanol have similar total (Hildebrand) solubility parameters of 25.1 and 26.1 $MPa^{0.5}$, respectively, but their affinities are very different. In this case, ethanol is water soluble and nitromethane is not. The sole use of the Hildebrand parameter would have precluded this determination [27]. In addition to the large amount of HSP currently available, a method of group contribution exists for prediction of individual solvent

parameters for components not yet determined. HSP can be calculated with a table of molecular group contributions and Equation 2.6

$$\delta = \left(\sum_i n_i F_i + \sum_j m_j S_j + 75954.1\right)^{0.383837} - 56.14 \qquad (2.6)$$

where F_i is the contribution of a first-order group of type *i* and n_i the number of times that *i* appears in the compound, and S_j is the contribution of second-order group of type *j* that appears m_j times. In addition to hand calculations, many computer programs are available to automate this process such as ThermoData Engine (TDE) provided within the ASPEN Plus software suite. TDE is a thermodynamic data prediction, evaluation, and correlation tool provided though a long-term collaboration agreement with the National Institute of Standards and Technology (NIST). This particular program accepts input of the molecular structure of the compound with key species properties such as molecular weight and specific gravity for parameter estimation. TDE utilizes twenty-eight predictive methods based on group contribution, corresponding states theory, and a library of electronic databases of experimental data. The primary focus of TDE is on pure organic compounds comprised of carbon, hydrogen, oxygen, nitrogen, fluorine, chlorine, bromine, iodine, sulfur, and silicon [28, 29].

Chapter 3

Experimental Details

This thesis is focused on material compatibility in passive two-phase immersion cooling applications. The research was conducted as part of a larger multidisciplinary project and some results herein involved other researchers. For example, radio frequency (RF) testing was carried out with Dr. Michael Hamilton's group in the electrical engineering department and small scale tank tests were conducted with Dr. Sushil Bhavnani's group in the mechanical engineering department, both at Auburn University. All other work not referenced was a product of the author's alone.

3.1 Soxhlet Extraction

Accelerated testing of component materials took place within a Soxhlet extractor. A portion of component material taking up approximately 30-40% of the thimble volume was placed within the Soxhlet apparatus; 120 mL of engineered dielectric fluid was added to the round bottom flask. The masses of the component material and round bottom flask were recorded before experiment initiation. The Soxhlet apparatus was assembled, placing the thimble within the extractor and connecting the round bottom flask and condenser to the extractor. Glass joints were sealed with Parafilm and the round bottom flask was covered in a sheet of insulation. The six-position Glas-Col heaters were set to a dial position of 4.5 which correlated to approximately 95°C, based on water tests. This

temperature setting maintained heated glassware and prevented early condensation of the engineered fluid within the vapor tube. It also helped to account for boiling point elevation as the contaminant concentration increased during accelerated testing. Figure 6 displays a typical Soxhlet setup used during the extraction process.

Figure 6. Twelve simultaneous Soxhlet extractions of component materials.

After extraction, the extraction apparatus was disassembled and the component material weighed. Three 20 mL extraction fluid samples were collected and the masses determined. These samples were collected specifically for general, pH, and RF testing. RF testing of contaminated samples was carried out via the previously mentioned collaboration [30]. The remaining extraction fluid was allowed to evaporate within an evaporation flask in order to determine the representative percentage of contaminant within the extraction fluid.

The round bottom flask was allowed to dry and the final mass was recorded. Figure 7 displays the typical sampling procedure. In some cases the accuracy of the mass balances were more important than the collection of extraction fluid. Here, sample collection was forgone and the extraction fluid was left within the round bottom flask to evaporate. The final mass of the round bottom flask was determined after complete evaporation of the extraction fluid.

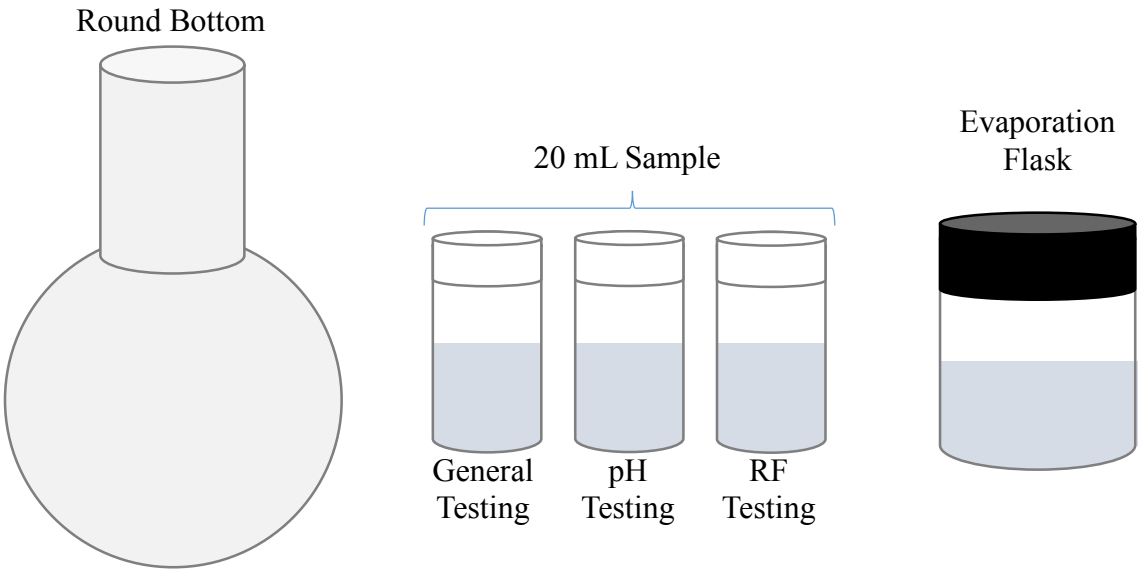

Figure 7. Sampling procedure.

3.2 Small Scale Tank Testing

In some cases, contaminated fluid was acquired from small scale tank tests conducted by collaborator Dr. Sushil Bhavnani. In those tests, printed circuit boards and Teflon insulated wiring were in direct contact with the dielectric fluid. Integrated circuit chips were powered in a four die configuration on a vertically-oriented printed circuit board. The chips were subjected to increasing and decreasing heat flux cycles, referred to

as data runs. Figure 8 provides a graphical depiction of the testing process and the tank testing setup itself. In a limited case, data runs were completed with intentionally contaminated Novec 649 fluid. These runs were completed to examine the effect severely contaminated fluid would have on the thermal performance of the system. To create the intentionally contaminated fluid, 30 mL of DOP were added to 8 L of Novec 649 yielding a concentration of 3.70 g/L or 0.23 wt% contaminants.

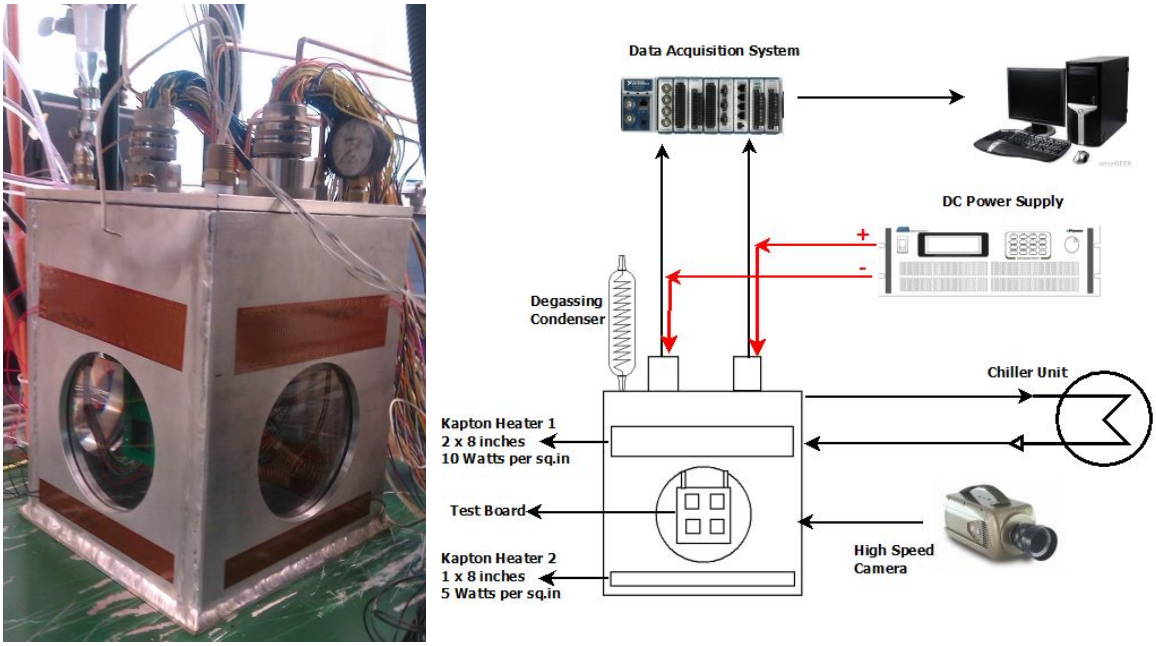

Figure 8. Tank testing apparatus and data acquisition diagram [31].

3.3 Mass Balances

A main source of data collected during accelerated testing was through the use of mass balances. This was a similar approach to that taken by 3M and others [7]. However, in the other cases, all dielectric fluid was allowed to vaporize from the distillation flask leaving behind only the contaminant substances. This resulted in less mass balance error

but prevented obtaining chemical or electrical information on the contaminated fluid. In this work, the sampling procedure was refined during initial experimental runs. A standard procedure was developed where three sample vials with 20 mL of contaminated fluid were taken from each accelerated test to be distributed for general analysis (e.g., ATR-FTIR), pH testing, and dielectric testing. The remainder of the fluid was set aside within an evaporation flask for quantification of the mass of contaminant (residue) removed from the material under extraction.

In order to determine the mass of the fluid within a sample vial or evaporation vial, the mass of the empty vial was subtracted from the mass of the full vial as shown in Equation 3.1.

$$m_{fluid,sample} = m_{sample,full} - m_{sample,empty} \tag{3.1}$$

The total residual mass of material extracted was determined by allowing the remaining fluid not consumed by the sample vials to evaporate within the evaporation flask. Subtracting the mass of the empty evaporation vial from the mass of the evaporation vial after allowing the fluid to evaporate yields the mass of the residue within the evaporation vial (Equation 3.2).

$$m_{residue,evap} = m_{evap,sample} - m_{evap,empty} \tag{3.2}$$

Next, the total residue extracted from the component was determined by dividing the mass of the residue within the evaporation flask by the weight percentage of the fluid added to the evaporation flask as shown in Equation 3.3. This weight percentage permits the estimation of the residue within the sample vials without having to allow them to completely dry.

$$m_{residue,total} = \frac{m_{residue,evap}}{w_{fluid,evap}} = \frac{m_{residue,evap}}{\frac{m_{fluid,evap}}{m_{fluid,total}}} \tag{3.3}$$

Finally, the mass extracted was calculated by subtracting the empty flask weight from the mass of the flask after extraction (i.e., containing residue) and adding the mass of the residue determined to be in the sample vials (Equation 3.4). This value was then divided by the total mass of the material initially to arrive at a percentage (Equation 3.5).

$$m_e = (m_{flask,residue} - m_{flask,empty}) + m_{residue,total} \quad (3.4)$$

$$m_{e\%} = \frac{m_e}{m_{material,intially}} \, x \, 100\% \quad (3.5)$$

In addition, the mass absorbed was determined in a similar manner by subtracting the initial mass of the material from the final mass of the material and adding the mass extracted (Equation 3.6). Again, this value was divided by the total initial mass to arrive at a percentage (Equation 3.7).

$$m_a = (m_{material,final} - m_{material,intially}) + m_e \quad (3.6)$$

$$m_{a\%} = \frac{m_a}{m_{material,intially}} \, x \, 100\% \quad (3.7)$$

3.4 Optical Microscopy

A Nikon (Melville, NY) Eclipse 80*i* optical microscope was used to examine the changes in surface characteristics of the component materials as well as study any particulates that showed up in the contaminate residues. Samples were illuminated with either reflected or transmitted light. Component material samples were prepared by placing them on a glass slide and residue samples were allowed to dry before viewing. A 20x (0.45 NA) Nikon "Luminous Universal Plan Fluor" objective was used either with a 1x or 2x magnification applied before the camera yielding a maximum effective magnification of 40x. Images were captured and processed in Nikon Elements software.

3.5 Scanning Electron Microscopy

A scanning electron microscope (SEM) was utilized for characterization of sample surface morphology. In addition, energy dispersive X-ray spectroscopy (EDS) was used in conjunction with SEM for elemental analysis. Samples were prepared by adhering double sided carbon tape to a JEOL Specimen Mount and pressing materials onto the surface of the carbon tape. Samples were then gold sputter coated to enhance their conductivity. Examination was carried out using a JEOL 7000-F Field Emission-Scanning Electron Microscope.

3.6 Ultraviolet-Visible Spectroscopy

Ultraviolet-visible spectroscopy (UV-Vis) is an analytical technique often used for the quantification of analytes such as organic compounds. UV-Vis is particularly useful for compounds that have π-electrons, non-bonding valence-shell electrons and/or a great deal of conjugation. This technique uses a range of wavelengths starting from the near UV range of 200-380 nm progressing through the visible wavelengths of 380-780 nm to 800 nm. Within this range, molecules undergo electronic transitions from a ground state to an excited state. The energy difference between these two excited states is equal to the energy of the photons absorbed by the molecule. UV-Vis spectra consist of broad absorption bands rather than sharp lines is due to the absorption of radiation over a range of wavelengths. Furthermore, the electronic transition can be accompanied by a change between the vibrational levels. Thus, photons that have excess or insufficient energy can be accepted by a molecule whether the molecule undergoes a pure electronic transition or a transition between vibrational levels [32].

Quantification of analytes is a particularly useful result obtainable from UV-Vis analysis. Concentrations of absorbing species are commonly determined utilizing the Beer-Lambert law shown in Equation 3.8

$$A = \log\left(\frac{I_0}{I}\right) = \epsilon c L \tag{3.8}$$

where I_0 is the intensity of incident light at a particular wavelength, I the intensity of transmitted light, ϵ is extinction coefficient, c the concentration, and L the path length. The extinction coefficient is a fundamental molecular property (directly measureable) for a particular solvent, specific for a particular wavelength, temperature and pressure [33].

UV-Vis was particularly useful for species containing conjugated ring structures and the non-bonding electrons found on oxygen. Polymeric additives such as plasticizers are organic species that encompass such structures. This particular technique was applied to dioctyl phthalate (DOP), a largely used plasticizer. The non-bonding valence shell electrons of oxygen present correspond to the first peak around 200 nm and the conjugated ring structure leads to the second peak around 275 nm. The structure of DOP and its UV-Vis absorbance spectrum are provided in Figure 9. Making use of these peaks, a calibration curve was created for quantification of DOP present within a component's residue. Some concentrations were diluted in order to maintain the absorption values within the linear region of the Beer-Lambert law.

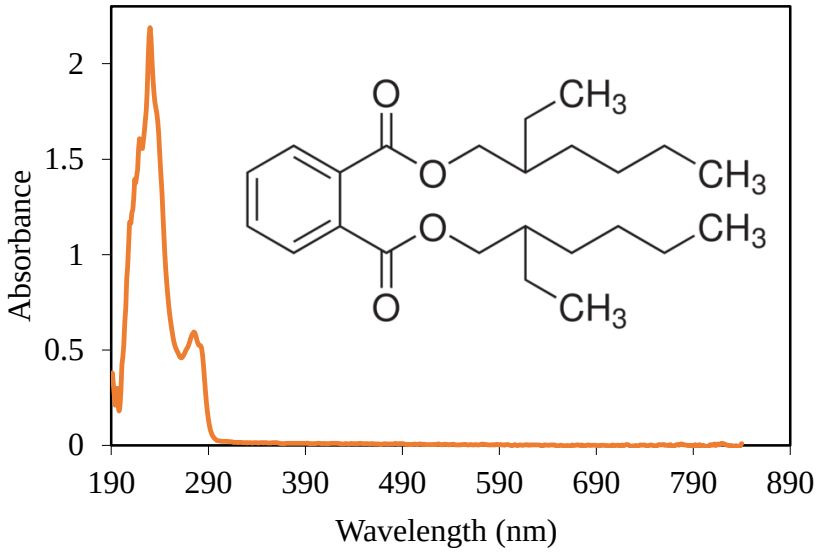

Figure 9. Chemical structure of dioctyl phthalate (DOP) and its UV-Vis absorption spectrum.

A stock solution of DOP in hexane was created. From this solution, samples were diluted to obtain a range of concentrations (weight fractions). These samples were placed within a 1 cm quartz cuvette and analyzed with UV-Vis. The absorbance at 275 nm was recorded. A plot of the absorbance values with weight fraction was produced and a linear line fitted to the data. Figure 10 shows the data and linear fit. The extinction coefficient was determined to be 1800.8 g total g DOP^{-1} cm^{-1}.

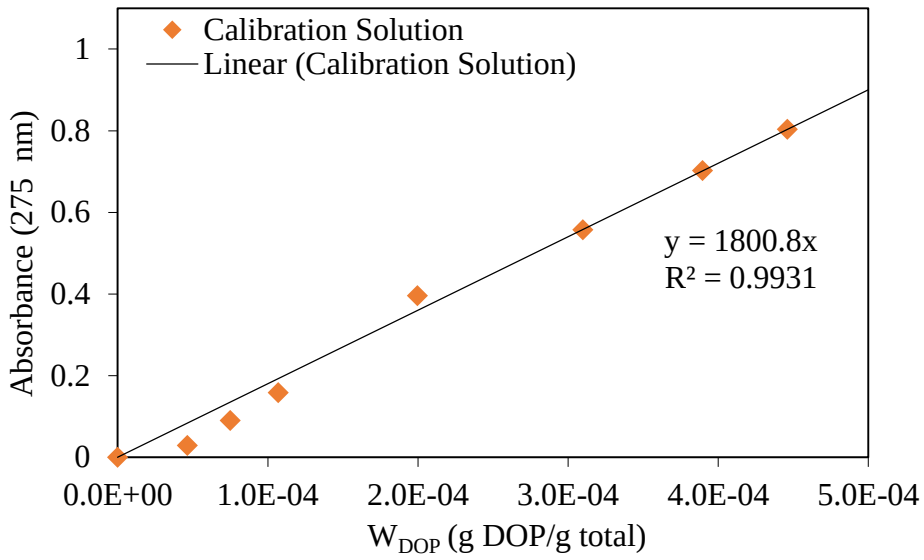

Figure 10. Calibration curve of DOP in hexane used for concentration determination.

UV-Vis spectroscopy was performed with a Thermo Scientific NanoDrop 2000c spectrophotometer with a 1 cm quartz cuvette. 1 mL of a component residue was allowed to dry within a sample vial, leaving behind the contaminant. 3 mL of hexane were added to the remaining contaminant and mixed with a Barnstead/Thermolyne Maxi-Mix Plus mixer. Masses were recorded for all fluid measuring steps and concentrations were determined via a calibration curve.

3.7 Fourier Transform Infrared Spectroscopy

Fourier Transform Infrared (FTIR) can be applied to all forms of samples whether solids, liquids, or gasses. FTIR passes infrared radiation through a sample and registers the radiation that passes through (transmitted). The result is a spectrum that represents the molecular fingerprint of the sample. This fingerprint can be used to qualitatively probe the

chemical composition and molecular structure of an unknown compound. Such determinations are typically made via comparisons of an unknown spectrum to a library of known compounds. For less common materials, FTIR can be coupled with mass spectrometry, X-ray diffraction, nuclear magnetic resonance, and various other techniques for positive identification. In addition, the size of the peaks within an FTIR spectrum directly correlate to the amount of material present, allowing for quantitative analysis [34, 35].

FTIR spectroscopy is based on the vibrational excitation of molecular bonds by the absorption of infrared light energy. A molecular bond can vibrate at several specific frequencies. These vibrational frequencies are caused by the absorption of infrared light energy. The light energy absorbed (determined by wavelength) is exactly equal to the difference between the two energy states – usually the ground state (E_0) and the first excited state (E_1) [36]. Consistent with the infrared portion of the electromagnetic spectrum, the energy associated with these (successive) transitions in molecular vibrational states is around 1-10 kilocalories/mole [35].

Originally, dispersive spectroscopy separated individual frequencies of energy via a prism or grating. The detector then measured the energy at each frequency that passed through the sample resulting in a plot of intensity versus frequency (spectrum). FTIR was developed to overcome the limitations of dispersive instruments such as slow scanning times. FTIR measures all of the frequencies simultaneously rather than individually though the use of an interferometer. As the infrared beam passes through the interferometer, a set of mirrors are used to cause wave interference that produces a resulting signal (interferogram) that contains information about every infrared frequency that comes from

the source. The raw data of absorption versus mirror position is collected and processed using a fast Fourier transform (FFT) algorithm to produce the spectrum [33].

Attenuated total reflectance (ATR-FTIR) makes use of a crystal (e.g., germanium, diamond, etc.) that observes total internal reflection. Upon impact of the infrared light with the surface of the crystal that is in contact with the sample, an evanescent wave is created that penetrates the sample. In regions of the IR spectrum where the sample absorbed energy, the evanescent wave will be altered or attenuated [33]. Any attenuated energy is passed back into the crystal from the sample and registered by the detector. ATR-FTIR is a critical technique used in the analysis of solid materials or small amounts of liquids.

In order to identify unknown compounds within residues of the extraction fluid, infrared spectroscopy was conducted. A Thermo Scientific Nicolet iS10 FTIR spectrometer was used in conjunction with a HATR diamond attenuated total reflectance crystal for full spectral range analysis from 4000 – 400 cm^{-1}. Two methods of sample preparation were conducted. The first method allowed extraction fluid samples to directly dry on the crystal whereas the second method allowed extraction fluids to condense within a sample vial. The remaining residue was swabbed and placed onto the ATR crystal for identification. The sample spectra were collected and analyzed within Omnic Series 8.1 software. Compound identifications were made with the OMNIC Spectra Advanced Material Characterization Software package containing over 9,000 spectra was well as literature searches.

3.8 Thermogravimetric Analysis

Thermogravimetric analysis (TGA) is a method of thermal analysis used to determine physical and chemical properties of materials as a function of increasing temperature or time. TGA is often used to examine the mass lost or gained due to decomposition as well as the loss of volatiles such as water or other fluids that may be absorbed or adsorbed. TGA is particularly useful in determining relative changes in these properties for a given experimental compound.

Thermal characterization of polymers and activated carbon was conducted using a TA Instruments Q50 Thermal Gravimetric Analyzer (TGA). Polymer samples were compared after extraction with all three engineered fluids. Samples were loaded into a tared platinum, high temperature weigh pan and the sample chamber was purged with both air and argon at a flowrate of 90 cm^3/min. The temperature was held at 10°C above the boiling point of the engineered fluids for twenty minutes and then ramped at 10°C/min to 100°C beyond the thermal degradation point of the polymer.

3.9 Differential Scanning Calorimetry

Differential scanning calorimetry (DSC) is a thermal analysis technique that measures the difference in the amount of heat required to increase/decrease the temperature of a sample and a reference. DSC is often used to detect phase transitions of samples such as melting, crystallization, or glass transition temperatures. In these instances, the heat flow required for these transitions will increase or decrease depending upon whether the process is endothermic (requiring heat) or exothermic (outputting heat). DSC is commonly used to examine the thermal characteristics of polymer materials. Thermal characterization

of polymeric component materials was conducted using a TA Instruments Q2000 differential scanning calorimeter (DSC). DSC studies were performed within hermitically sealed aluminum pans at a scan rate of 10°C per minute over a temperature range of -90 to 300°C with three thermal cycles of heating-cooling-heating.

3.10 Gas Chromatography-Mass Spectrometry

Samples were prepared for gas chromatography-mass spectrometry (GC/MS) by first allowing the component residues to completely dry within a sample vial. This allowed for a condensed sample to be reconstituted within acetonitrile for injection into a Waters GCT Premier mass spectrometer. The GCT Premier is an orthogonal acceleration time-of-flight (oa-TOF) mass spectrometer housed within the Mass Spectrometry Center and maintained under the College of Sciences and Mathematics located on Auburn University's campus. Spectrum analysis was conducted using Masslynx (V4.1: SCN 569) software with compound matches made to NIST/NIH/EPA Mass Spectral Library for positive identification. Samples were ionized via electron ionization (EI) and passed through a ZB-5MS, 30 mm x 0.25 mm x 0.25 μM (length x diameter x coating), Phenomenex column with a helium carrier gas.

Chapter 4

Results and Discussion

4.1 Soxhlet Screening Study

The individual component materials chosen for investigation are listed in Appendix A – Materials Included in Screening Study. These materials were subjected to an accelerated testing procedure entailing a standardized five day Soxhlet extraction. Samples were numbered for identification purposes and followed the format: (Identification #) Material Name. Upon completion of extraction, mass balances were calculated for the amount of material, termed residue, removed from the component material and analysis was conducted to determine the chemical makeup of the eluted compounds. Where possible, concentrations were calculated for the residues found in solution.

4.1.1 Error Estimation

Twelve Soxhlet extractions of 4.34 grams of (21) PVC were carried out in Novec 649. The mass extracted and mass absorbed data, along with some basic statistical figures, are provided in Table 5. The standard deviation was found to be 0.80% and 0.40% for the mass extracted and mass absorbed (absolute value) calculations, respectively. Error was estimated as two standard deviations yielding ± 1.60% for mass extracted and ± 0.80% for mass absorbed. Ideally, extractions on all materials would have been repeated multiple

times in order to develop confidence in the data obtained. However, the number of materials named for testing combined with the length of extraction and cost of materials/fluids made this impractical. In a limited case, some materials were extracted more than once in Novec 649. These materials and the standard deviations of masses extracted and absorbed are shown in Table 6. It was expected that component materials would elute compounds at differing rates dependent on thermodynamic interactions and diffusion kinetics. However, comparison of the estimated error from repeated PVC extractions is similar to that of materials only extracted a few times. The large difference determined in (18) Tygon is likely due to its composition containing a greater amount of leachables.

Table 5. Soxhlet error determination of masses extracted, masses absorbed, and concentration with (21) PVC in Novec 649.

Sample #	$m_{e\%}$	$m_{a\%}$	Concentration (g/L)
1	2.10%	0.10%	0.525
2	2.60%	0.20%	0.732
3	4.50%	1.50%	0.361
4	2.70%	0.00%	0.661
5	3.50%	0.10%	0.488
6	4.00%	0.70%	0.706
7	2.10%	0.00%	0.294
8	2.90%	0.90%	0.513
9	1.70%	0.40%	0.585
10	2.30%	0.10%	0.810
11	2.50%	0.20%	0.691
12	2.40%	0.20%	0.145
Std. Dev.:	0.80%	0.40%	0.198
Average:	2.78%	0.37%	0.543
Max:	4.50%	1.50%	0.810
Min:	1.70%	0.00%	0.145
Range:	2.80%	1.50%	0.665
Std. Error:	0.24%	0.16%	0.057

Table 6. Standard deviation of masses extracted and absorbed for some materials extracted more than once.

Material		Standard Deviation		Number of Extractions
#	Name	$m_{e\%}$	$m_{a\%}$	
18	Tygon	8.19%	8.80%	3
20	EPDM	0.55%	0.66%	3
24	Nalgene	0.25%	0.06%	3
25	Natural Rubber	0.21%	0.26%	3
26	Latex Rubber Tubing	0.40%	0.29%	3
	Average:	1.92%	2.01%	
	Max:	8.19%	8.80%	
	Min:	0.21%	0.06%	

The standard deviation of the concentration data provided in Table 5 was found to be 0.198 g/L. This is significantly large given that the minimum amount of DOP concentration determined was 0.145 g/L. This raises question on the accuracy of the procedure for determining concentration. A large assumption is made during the concentration calculation that the DOP within the sample vial is of negligible mass or volume. Essentially, the amount of DOP added to the hexane is an insignificant amount compared to the much larger amount of solvent added. This is a reasonable assumption as the weight of DOP left in a vial after evaporation of 1 mL of fluid sample (i.e., Novec 649, HFE-7100, FC-72) is not easily determined via a scale due to the small amount that remains.

Another point to note is that the larger concentrations determined do not necessarily coincide with the larger mass extracted percentages. This indicates there is a discrepancy between the concentration being determined and the mass extracted which should be connected. It is believed that during collection of the sample that was to be used for concentration determination, contaminant (e.g., DOP) that was freely floating (i.e., super

saturated solvent) may have been pulled into the syringe and deposited into the sample vial producing an egregiously large concentration. This type of error was unavoidable for contaminants that were extracted to the extent DOP was. The average concentration of 0.543 g/L is probably a reasonable estimation of the amount of DOP extracted from (21) PVC with Novec 649 since most concentrations fall around the 0.500 g/L point.

The main source of error was believed to be the rapid evaporation of the solvent during sample collection and via leakage at the Soxhlet setup joints. Several remediation strategies were attempted such as sealing the joints with aluminum foil tape over traditional Parafilm as well as a Parafilm-Teflon tape-Parafilm layering technique. Figure 11 shows the aluminum foil tape over Parafilm at the round bottom flask/extractor joint as well as the traditional Parafilm setup. The attempted remediation strategies did not produce a noticeable decrease in solvent leakage. With aluminum foil, it was believed that the Parafilm prevented proper sealing of the connections by forming a barrier between the glass and the foil tape. This provided a route of escape even with the foil tape on top. In addition, the dielectric fluids' chemical structure similarity to Teflon prevented this tape from being used alone. Upon use of this tape in conjunction with Parafilm, the Parafilm appeared to overheat from the insulation of the Teflon tape and thus prevent a good seal around the glassware junctions.

Figure 11. Efforts to avoid joint leakage showing aluminum foil tape (bottom) over traditional Parafilm (top).

4.1.2 Mass Balances

For all materials subjected to accelerated testing, mass balances provided a key source of information regarding the movement of material within the system. It was simple to pick out the component materials that displayed the greatest amount of leaching. These materials were often polymeric in nature and represent the focus of the majority of analysis conducted. Figure 12 and Figure 13 display the masses extracted and absorbed, respectively, for the majority of materials. In most cases, the differences in material extractions and/or absorptions are not statistically different.

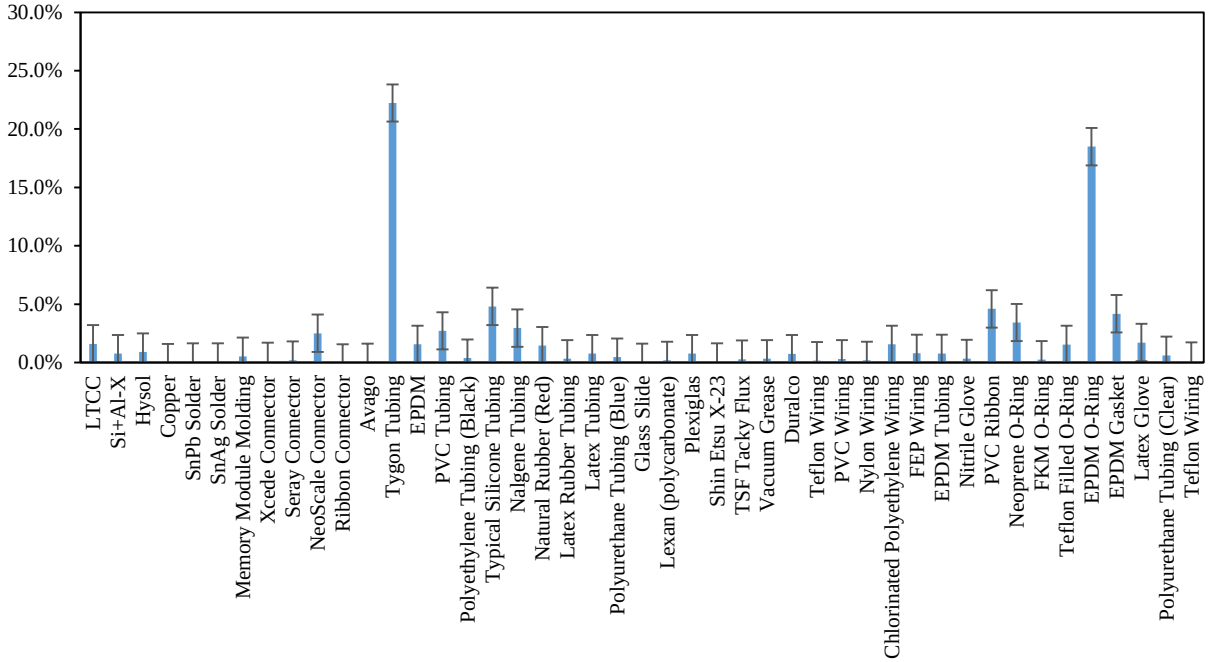

Figure 12. Mass extracted percentages of component materials subjected to accelerated testing in Novec 649.

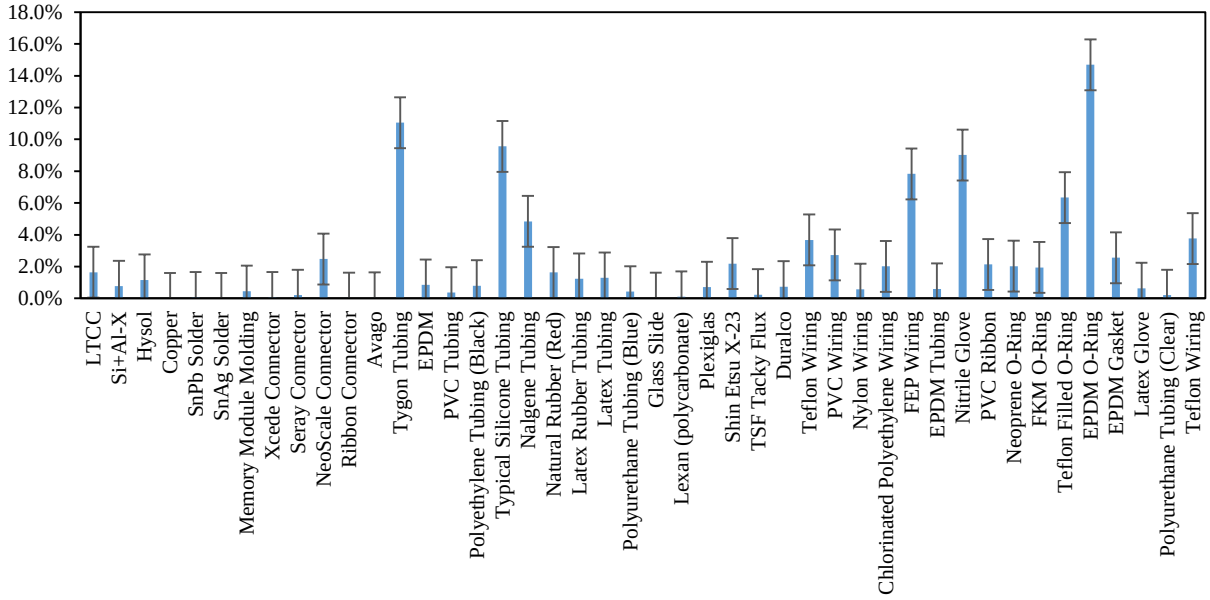

Figure 13. Mass absorbed percentages of component materials subjected to accelerated testing in Novec 649.

As previously mentioned, increasing the amount of post-Soxhlet residue sample available for analytical testing decreased the accuracy of the mass balance. In the standard Soxhlet test performed by 3M and others, all fluid was evaporated directly from the Soxhlet. This makes the mass balance simple, however, it precludes measuring fluid properties and leaves any residue distributed over a relatively large, somewhat inaccessible surface area. Removing fluid samples for analysis and evaporating off a portion of the fluid in a smaller container increased mass balance measurement error. Data on the mass change of the component material under study was generally less accurate than measurements of the amount of material extracted into the fluid. This was due to an initial amount of Novec 649 absorbed into the component which was rapidly evaporating during efforts to make final mass measurements. It was therefore difficult to assess the amount of initial absorption/swelling that existed during immersion. Similarly, more tightly adsorbed Novec 649 can compensate for the loss of additives/plasticizers during testing.

In order to evaluate the change in fluid contamination with time, studies were performed to examine the extraction rates of some component materials. Samples were collected from a sample collection port installed in the side arm of the round bottom flasks. The setup for this experiment is shown in Figure 14. A 3.4 g sample of (21) PVC tubing was extracted in Novec 649 and HFE-7100 for twelve hours with two hour sample intervals. (21) PVC tubing was chosen given the ability to determine concentrations via UV-Vis. The results are shown in Figure 15.

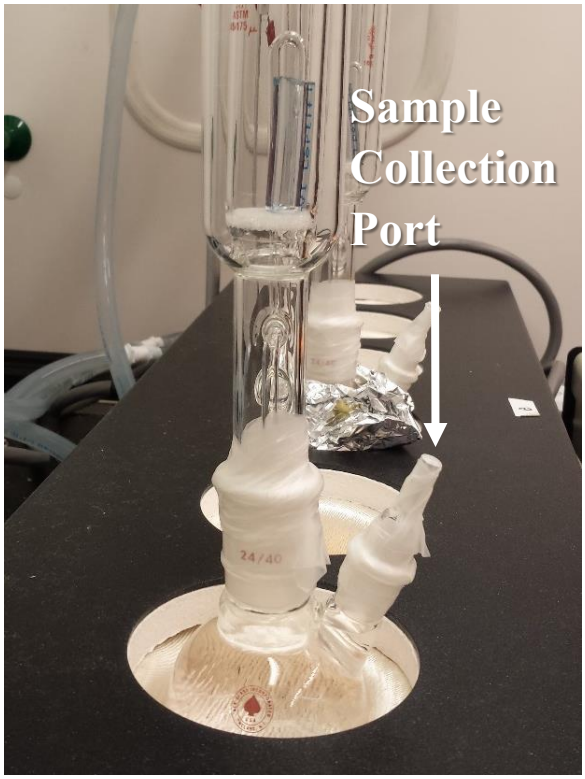

Figure 14. Soxhlet extraction of (21) PVC apparatus setup for concentration profile determination.

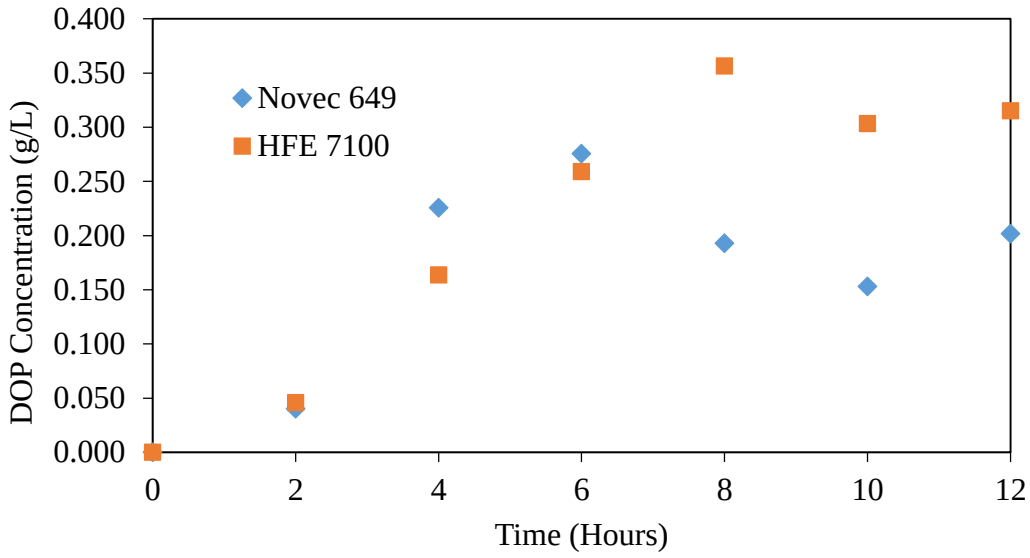

Figure 15. Concentration of DOP within Soxhlet setup during extraction of (21) PVC with Novec 649 and HFE-7100.

There was an initial increase in the concentration determined with time for both fluids, however, after the six hour point there was more scatter in the data. The rate of extraction was also clearly lower than in the first few hours. The error was determined to be a result of the Soxhlet extractor's status with regard to the number of times the thimble containing the material had emptied and been refilled with fresh fluid. Attention was not given to the Soxhlet extractor's turnover status during sample collection in order to preclude bias. A simpler method might entail counting extractor turnover and determining concentrations after a given number of refreshes. The amount of turnover for a given hour period could be determined and extrapolated for interval determination. Although this method could have led to a greater understanding of the transport kinetics involved and perhaps the barrier properties of the polymer, these analyses were outside the scope of the project. Further investigation would be necessary in order to develop a better understanding of the transport processes at hand. Feldman has explained these processes to be dependent upon many factors such as the physical properties of the polymer (e.g., density, solubility, morphology, etc.), nature of the fluid, and temperature among others [37].

A second approach was tested in which the concentration profile was split into twenty-four hour increments and three Soxhlet setups were initiated for each interval. This method did not provide the detailed information of the aforementioned procedure but instead provided a general consensus of the effect prolonged exposure to the dielectric fluids would have on the component materials. In addition, increasing the interval decreased the amount of error. Again this experiment was carried out with (21) PVC tubing

and Novec 649. Figure 16 shows the mass extracted and mass absorbed data for the first five days of extraction as well as two, four, six, and eight week intervals.

In some instances where extraction took place over many weeks it was necessary to replenish fluid that escaped out at the glass joints. As previously mentioned, it was difficult to properly seal the extraction apparatus given the chemical makeup of the engineered fluids. The Soxhlet apparatus was refilled through the opening at the top of the condenser while extraction was continually carried out. This replenishing had no effect on the final data collected given the use of pristine fluid. All of the contaminants extracted to this point remained within the evaporation flask per the design of a Soxhlet extraction apparatus.

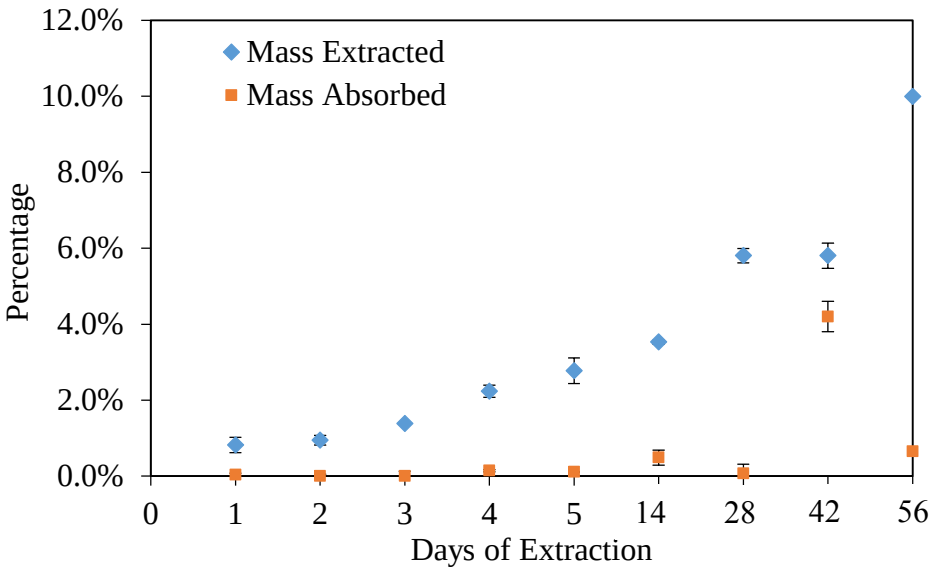

Figure 16. Mass extracted and mass absorbed data for the first 5 days of extraction and two week intervals up to 8 weeks.

The mass absorbed data on Day 42 is believed to be an outlier, since none of the other data from any of the accelerated testing experiments suggest significant absorption

by PVC. Ideally, to investigate the possible error, this instance would have been repeated but given the substantial cost of such a prolonged experiment its significance was not justified. The nearly exponential increase in the mass extracted was transport and thermodynamically driven. Since there is a finite amount of DOP present in the PVC, there cannot be a true exponential trend. Eventually the data would need to level off, however, obtaining the long term data is problematic. Interestingly, 3M data indicates that forty-eight hours is enough time to remove most of the extractables from elastomeric samples approximately 1 mm in thickness [7]. It is difficult to corroborate their information since larger amounts of component material were experimented on (around 4.34 g) and the geometry of the (21) PVC tubing was not accounted for.

From hexane extraction, it was determined that the total amount of DOP within a representative sample of (21) PVC tubing was around 36.4% which suggests that approximately one-third of the total DOP was extracted in the first 56 days [13]. For comparison, a 50% plasticizer content achieves sufficient flexibility for use in shower curtains [11, 14]. It was also found that the amount of DOP extracted during a five day exposure period depended upon the geometry of the PVC. Figure 17 shows the 14% difference between a piece of PVC that was extracted unaltered (whole) and a piece that was cut into smaller (ground) portions. It was believed that the amount of DOP extracted in a given amount of time would increase with decreasing size of the PVC portions. It was also reasonable to believe that the time for extraction would decrease with decreasing sample size (or increasing specific surface area) due to the reduced diffusion path length, assuming miscible materials. Although the geometry of the PVC played a significant factor in the amount of DOP extracted from the sample with hexane, this was not the case for

Novec 649. Figure 17 shows that the mass extracted remained 0.8% regardless of the geometry. This result is likely due to the low solubility of DOP in Novec 649, limiting the driving force for diffusion.

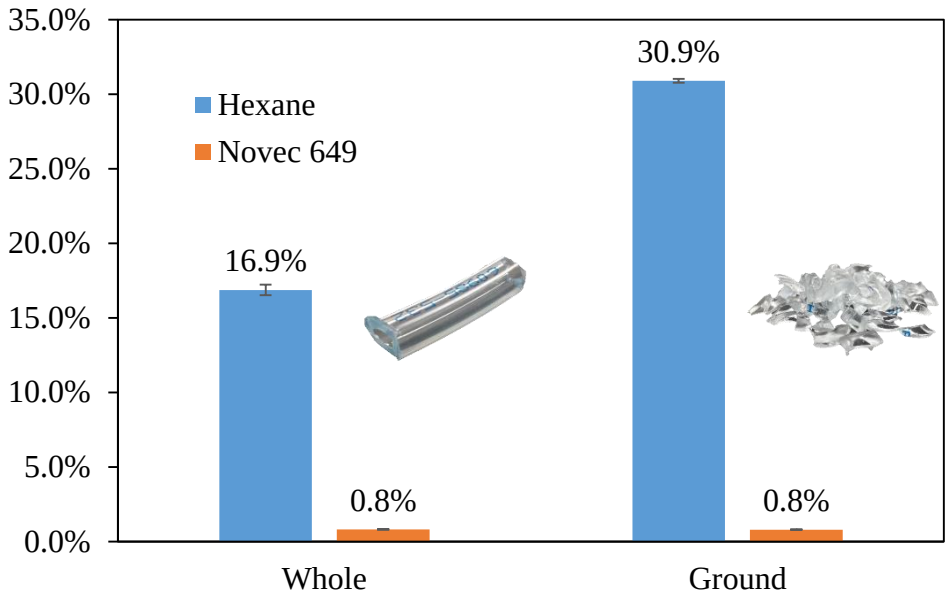

Figure 17. Passive extraction of (21) PVC tubing via hexane and Novec 649.

The results of the four week (extended) Soxhlet extraction of (18) Tygon tubing, (21) PVC tubing, (24) Nalgene tubing, and (39) Teflon wiring insulation were compared to those of the standard five day extraction testing. These materials were chosen to provide a range of polymers with different chemical makeup and different physical attributes without having to conduct four week studies on all materials. For example, Tygon was chosen for its likelihood to show high extraction and Teflon for its inertness. In addition, PVC is widely used and the concentrations of DOP extracted are readily determinable. Nalgene was chosen for its lower extraction. These extended extractions took place in all three dielectric fluids. There were no noticeable visual differences in the materials

extracted in the extended runs compared to those extracted for five days. For example, (18) Tygon tubing showed slight cloudiness on the end of the sample that was not submerged in fluid, similar to that found during five day testing. All of the polymers did appear to be more rigid and resistant to flexing, more so than that seen from the standard five day extraction. Comparisons of mass extracted and mass absorbed were made with the standard five day extraction data. These comparisons can be seen in Figure 18 and Figure 19. Comparing the four week test data with that of the five day test data, it is difficult to state any trends as most differences fall within the estimated error.

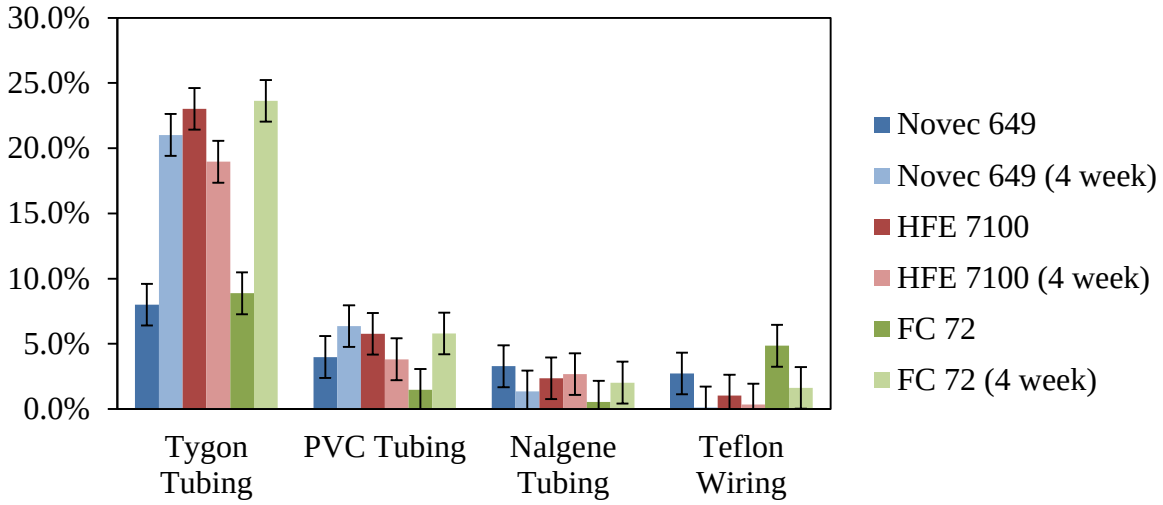

Figure 18. Comparison of mass extraction data from extended four week test and five day test.

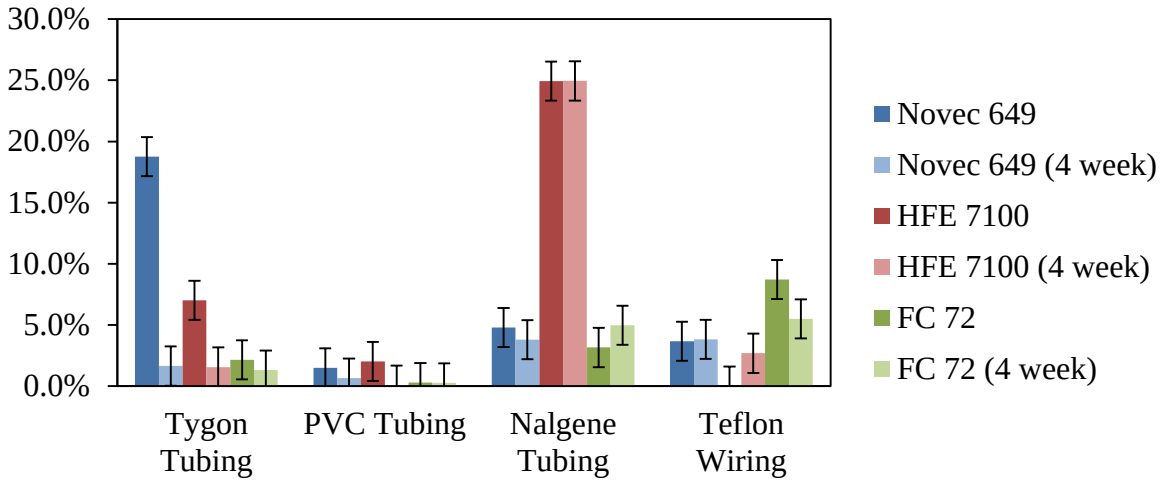

Figure 19. Comparison of mass absorption data from extended four week test and five day test.

4.1.3 Fluid Comparison

The experimental results from the Soxhlet extractions showed that materials experienced significantly different interactions with the three dielectric fluids. For example, (44) EPDM rubber tubing produced a residue that was bright yellow in color upon extraction with HFE-7100. Figure 20 displays a comparison to other materials undergoing extraction with HFE-7100 as well as (44) EPDM under extraction with FC-72. The sample undergoing extraction with FC-72 shows a cloudy fluid within the round bottom flask, consistent with extraction of other soft component materials, including other EPDM materials. The results observed with (44) EPDM rubber tubing are consistent with the prevailing trends observed. Typically, softer more pliable materials appear to contain greater amounts of leachable components and tend to yield greater amounts of contaminants in the collected residues, while physically harder materials tend to yield significantly less contaminants.

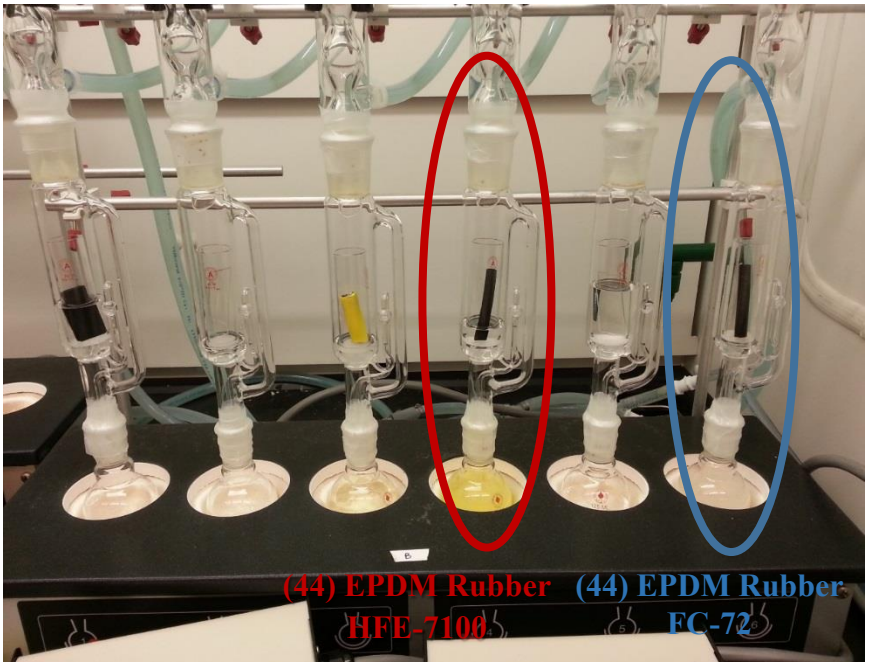

Figure 20. (44) EPDM rubber tubing undergoing extraction with HFE-7100 and FC-72.

Figure 21 displays the fluid residues of (26) latex rubber tubing after extraction in all three fluids. The HFE-7100 sample shows greater turbidity than the other two fluid samples - indicative of greater extraction. The masses extracted were determined to be 0.1%, 2.1%, and 0.1% for Novec 649, HFE-7100, and FC-72, respectively. Given Novec 649 and FC-72 have a similar physical structure, these results were in line with those expected.

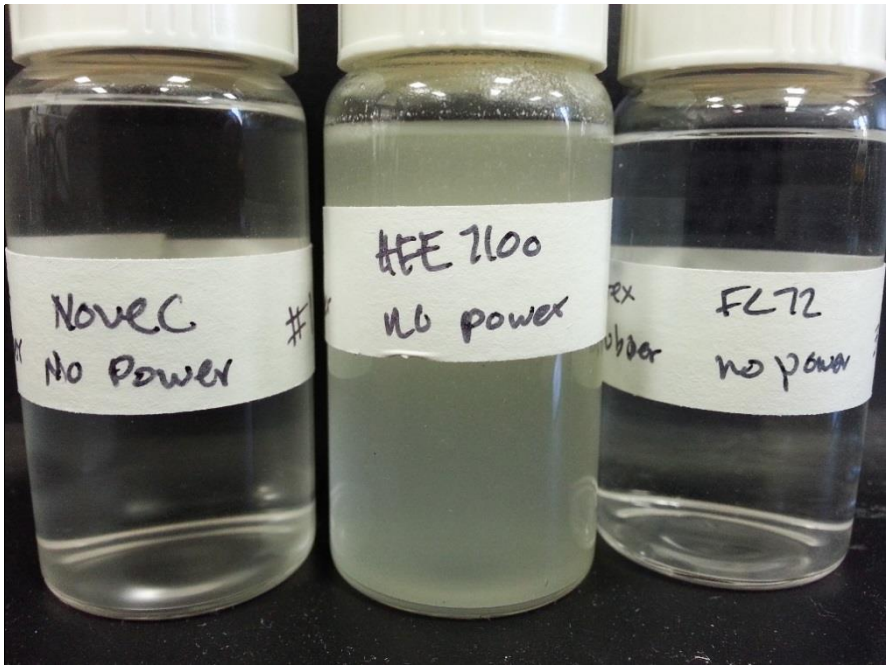

Figure 21. Fluid residues of (26) latex rubber tubing after extraction in Novec 649 (left), HFE-7100 (center), and FC-72 (right).

In order to develop a better understanding of the interaction of the three fluids with the various components, four benchmark polymeric materials were chosen for the ease of comparison. Again, these materials included (18) Tygon tubing, (21) PVC tubing, (24) Nalgene tubing, and (39) Teflon wiring insulation. It was expected that HFE-7100 would show the greatest amount of extraction followed by Novec 649 and then FC-72 based upon the KB values and physical structures of the fluids. This expected trend was not observed in every case. Figure 22 and Figure 23 show the masses extracted and absorbed, respectively. The values obtained for Teflon in the presence of the three fluids are a direct result of the fluid structures. FC-72 has a chemical structure very similar to that of Teflon; this facilitates fluid transport and increases solubility. Although FC-72 is often viewed as inert and has a KB value of 0, it does maintain the ability to extract plasticizers given the creation of a concentration gradient within the Soxhlet extraction apparatus. This in

conjunction with previous investigations of passive two-phase immersion cooling with FC-72, suggests that some level of contamination is tolerable within high performance computing applications.

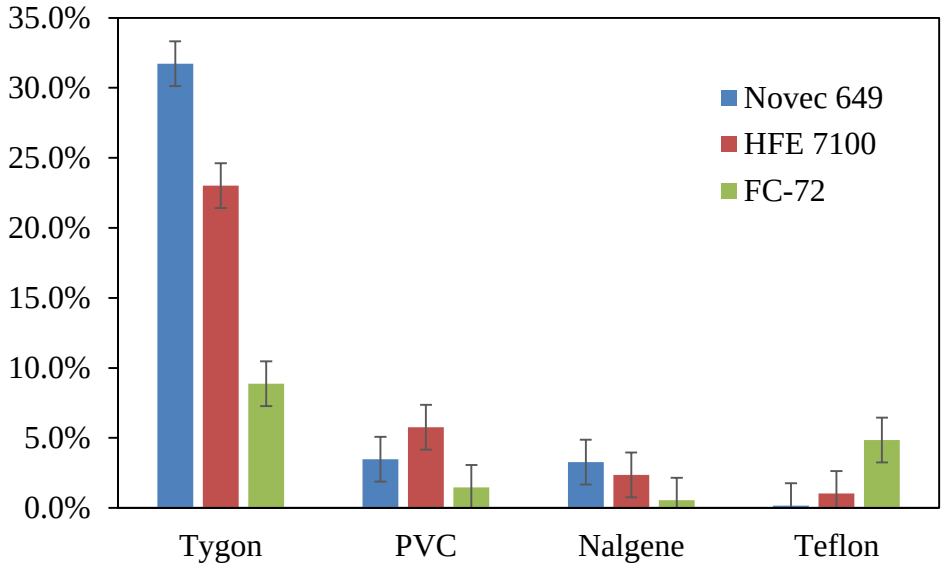

Figure 22. Mass extracted of component materials in all three dielectric fluids.

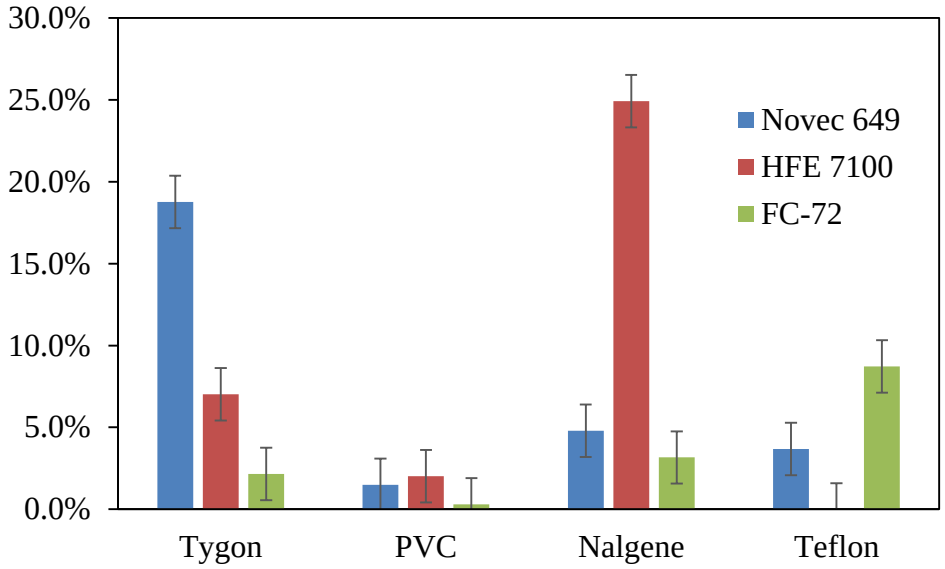

Figure 23. Mass absorbed of component materials in all three dielectric fluids.

ATR-FTIR spectral matching was used to verify that the materials extracted with FC-72 were the same as those extracted by Novec 649. Spectral matching cannot quantify

the amounts of component present, but can provide the likelihood that a given compound is present. As shown in Table 7, matching spectra from Novec 649 and FC-72 yielded similar results as to which components were present. The dominant materials were plasticizers or other additives. The presence of DOP plasticizer within Tygon and PVC tubing was expected and the identification of poly(ethylene:propylene:diene) and thermoplastic elastomer are believed to be the result of unbound monomer.

Table 7. Contaminant comparison of materials extracted with Novec 649 and FC-72.

Item #	Item	Contaminant	Match %	
			Novec 649	FC-72
18	Tygon tubing	Dioctyl Phthalate	57.28	91.63
20	EPDM	Poly(Ethylene:Propylene:Diene)	94.55	90.33
20-1	EPDM Gasket	Thermoplastic Elastomer	95.80	94.70
21	PVC Tubing	Dioctyl Phthalate	86.13	93.31
24	Nalgene Tubing	Silopren E 3078	90.05	91.15
		Silopren E 3096	89.93	89.88
		Poly(Dimethyl Siloxane)	85.97	86.66
25	Natural Rubber Tubing	Thermoplastic Elastomer	96.45	94.99

Some components were extracted in more than one fluid to develop a benchmark against FC-72. Figure 24 and Figure 25 provide a comparison of the masses extracted and absorbed for the components in the three fluids, respectively. A general trend that is further substantiated from Figure 24 is the more pliable materials typically show greater extraction percentages such as (18) Tygon tubing, (20) ethylene propylene diene monomer (EPDM), (21) PVC tubing, and (23) silicon pump tubing. This can be attributed to the fact that these polymers typically contain more plasticizer which is unbound and free to migrate out of

the polymer. (18) Tygon tubing is one of the more pliable materials under study and showed the highest mass extracted, as expected.

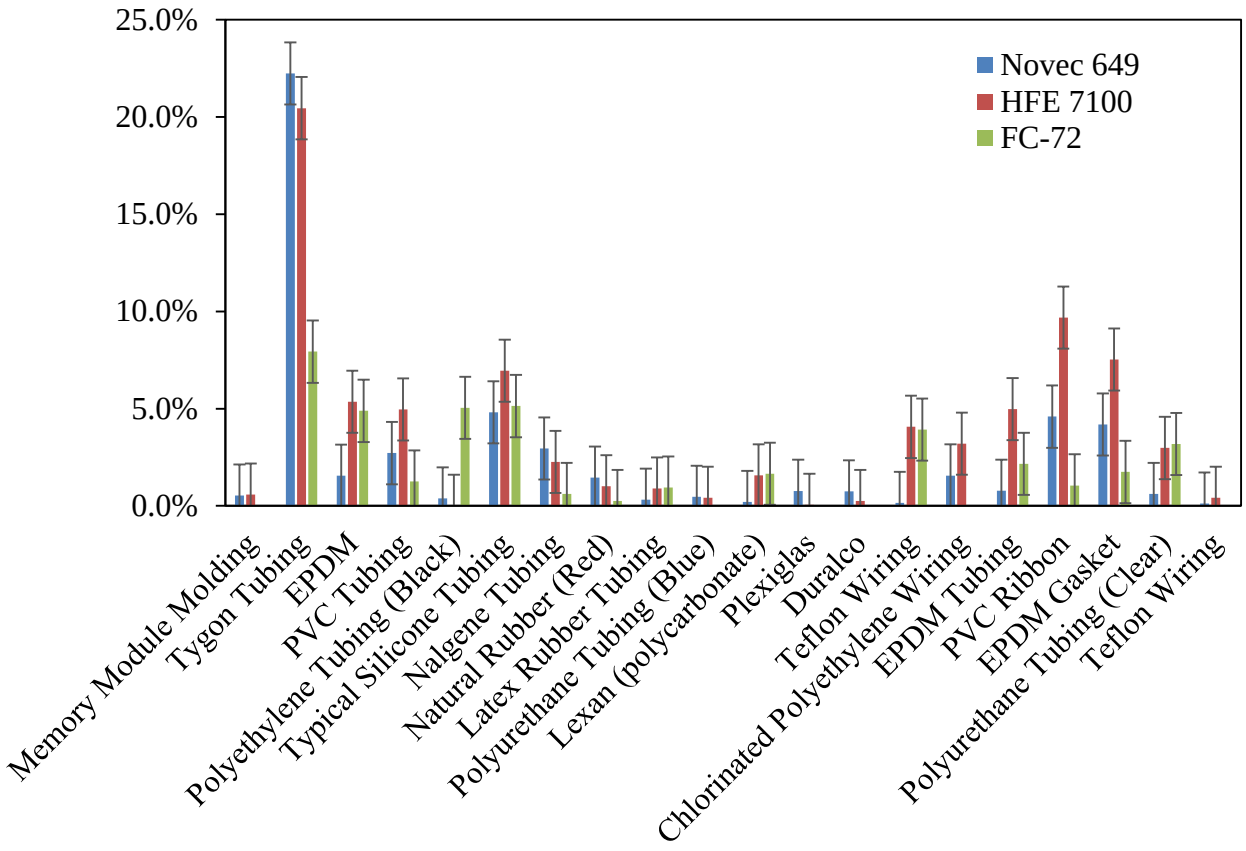

Figure 24. Comparison of masses extracted in all three fluids.

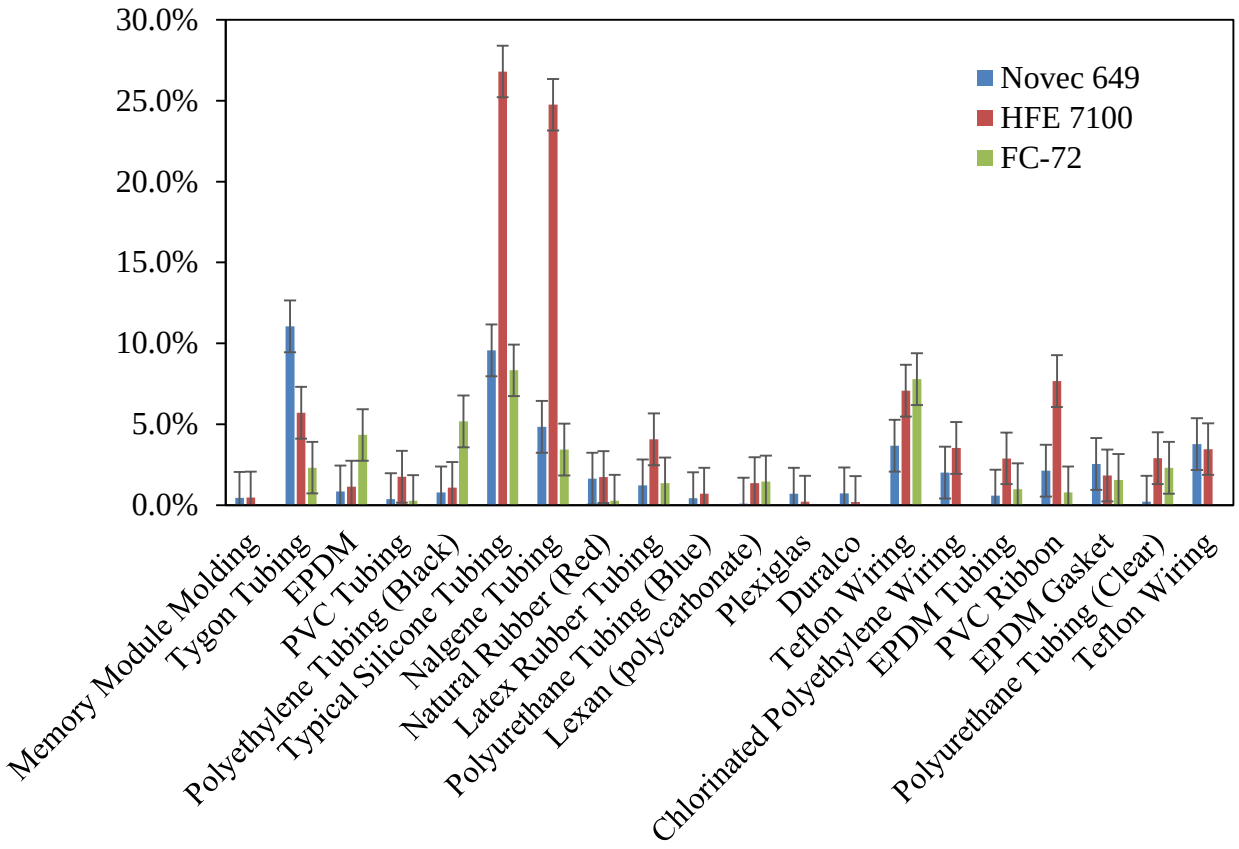

Figure 25. Compilation of component mass absorbed in all three fluids.

4.1.4 Effects of Immersion on Components

In addition to the changes seen in the dielectric fluids after accelerated testing, physical changes to the components themselves were sometimes also observed. Many materials showed no obvious changes under optical microscopy, however, a few materials showed changes that were very apparent to the naked eye. These changes were seen in the polymeric materials with the greatest masses extracted and primarily after extraction with HFE-7100. Figure 26 shows a comparison of (24) Nalgene after extraction with HFE-7100; the portion of material that was submerged within the fluid shows a color change compared with the material that was not submerged. Figure 26 also shows the physical

change of (18) Tygon after extraction with HFE-7100. This material became very opaque and exhibited a significant reduction in its pliability when compared to the original material.

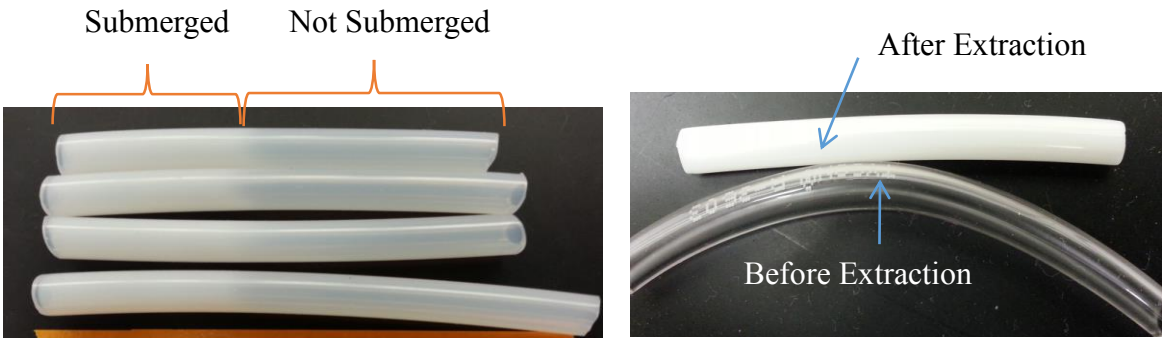

Figure 26. (24) Nalgene tubing (left) and (18) Tygon tubing (right) after extraction with HFE-7100.

Another example of the macroscopic changes seen in the physical appearance of component materials was identified after accelerated testing of (29-1) polyurethane tubing. (29-1) Polyurethane tubing was used for fluid transport within a small scale tank testing environment due to its low mass extraction and absorption figures. The initially acquired sample of polyurethane was colored blue as shown in Figure 27. The tubing acquired for fluid transport was instead clear. After extraction with all three dielectric fluids (Novec 649, HFE-7100, and FC-72), the sample exposed to Novec 649 exhibited a change in color. Yellowing in polymers is typically indicative of a degradation reaction. Singh, et al. have demonstrated yellowing within polyurethane coatings as a result of the formation of chromophores such as quinones and stilbenequinones through photo-oxidation [38]. Figure 28 shows a comparison of the samples after extraction in all three fluids. It should be noted that no color change was observed in the fluid, and based on pH measurements

there were no indications of acid formation in Novec 649. ATR-FTIR was conducted on all three sample residues. The results were similar to the sample that was initially obtained for accelerated testing, (29) polyurethane tubing (blue). Since the yellowing was not observed with the blue tubing, these results suggest that coloring agents may mask changes taking place in the material. It is also possible that the blue tubing may have contained additional stabilizers.

Figure 27. Originally acquired sample (29) polyurethane tubing (blue).

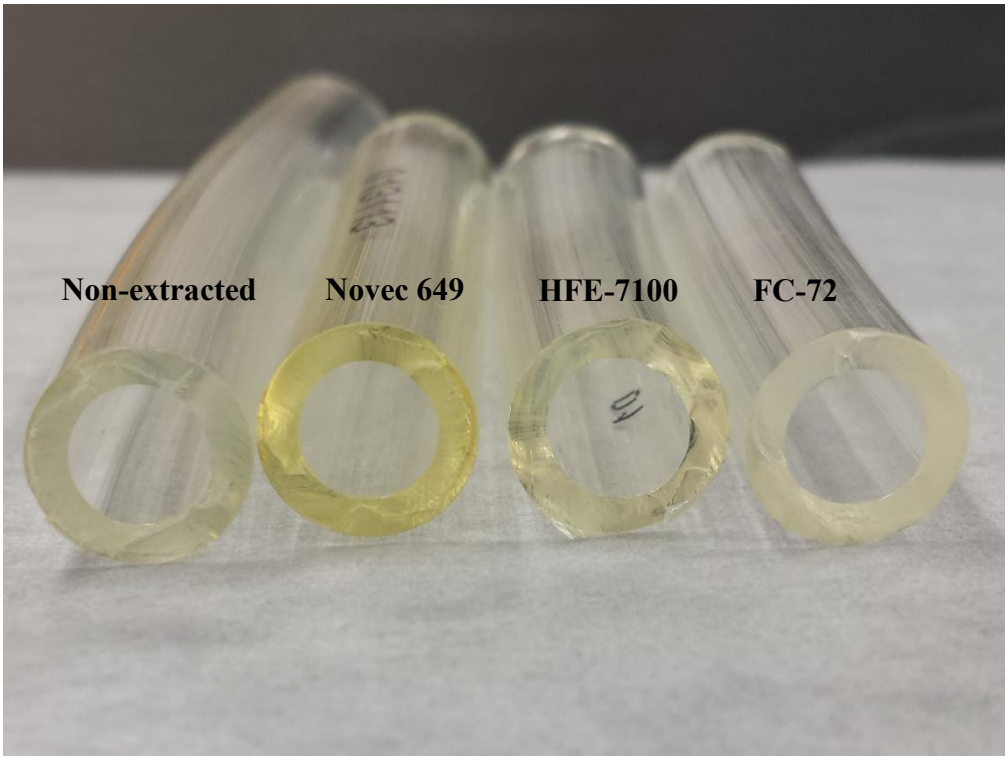

Figure 28. Sample comparison of (29-1) polyurethane tubing after extraction with all three dielectric fluids and a non-extracted control.

Thermal characterization was used as an additional means of exploring potential degradation for selected materials. Figure 29 shows the DSC thermogram of (29-1) polyurethane tubing after extraction with Novec 649 and HFE-7100 against a non-extracted control. Figure 30 and Figure 31 show the linear integration of each run's crystallization peak and melting peak, respectively. There was no significant change in total heat of crystallization or melting.

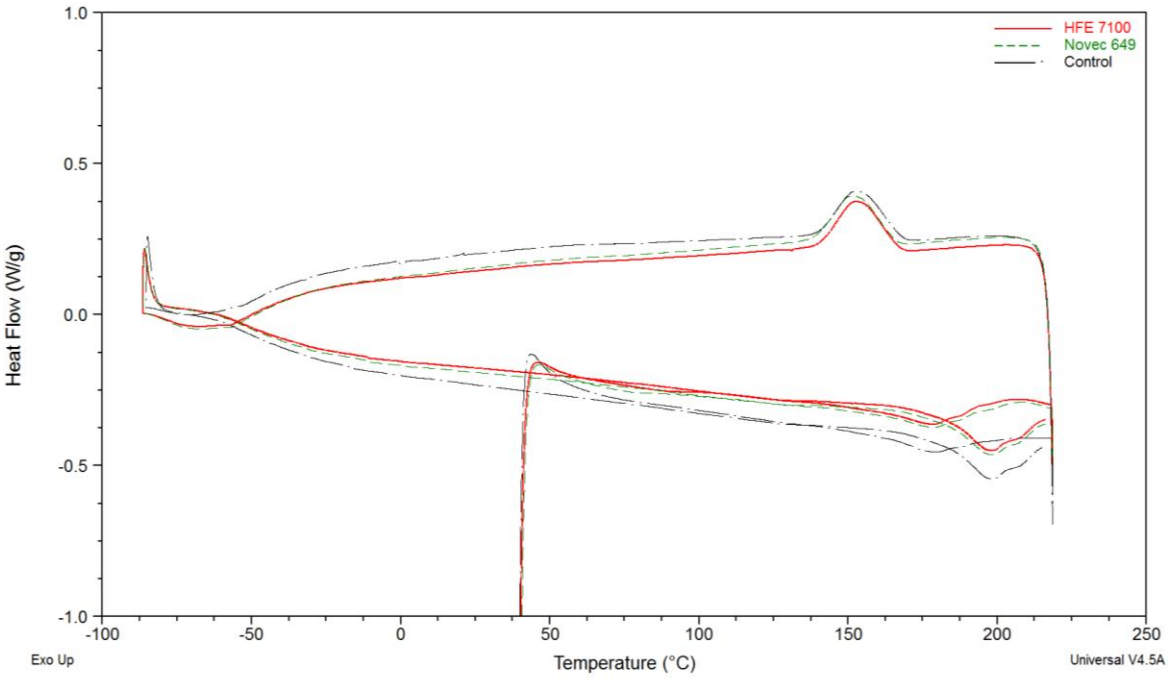

Figure 29. DSC thermogram of (29-1) polyurethane tubing after extraction with Novec 649 and HFE-7100.

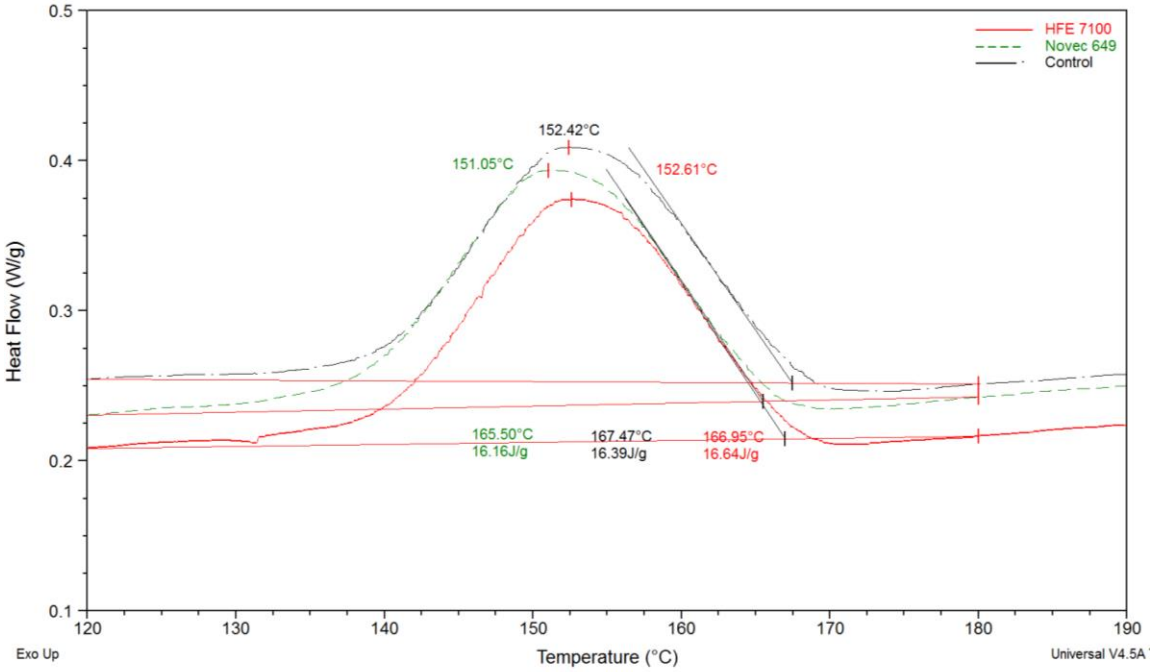

Figure 30. Linear integration of (29-1) polyurethane crystallization peaks after extraction with Novec 649 and HFE-7100.

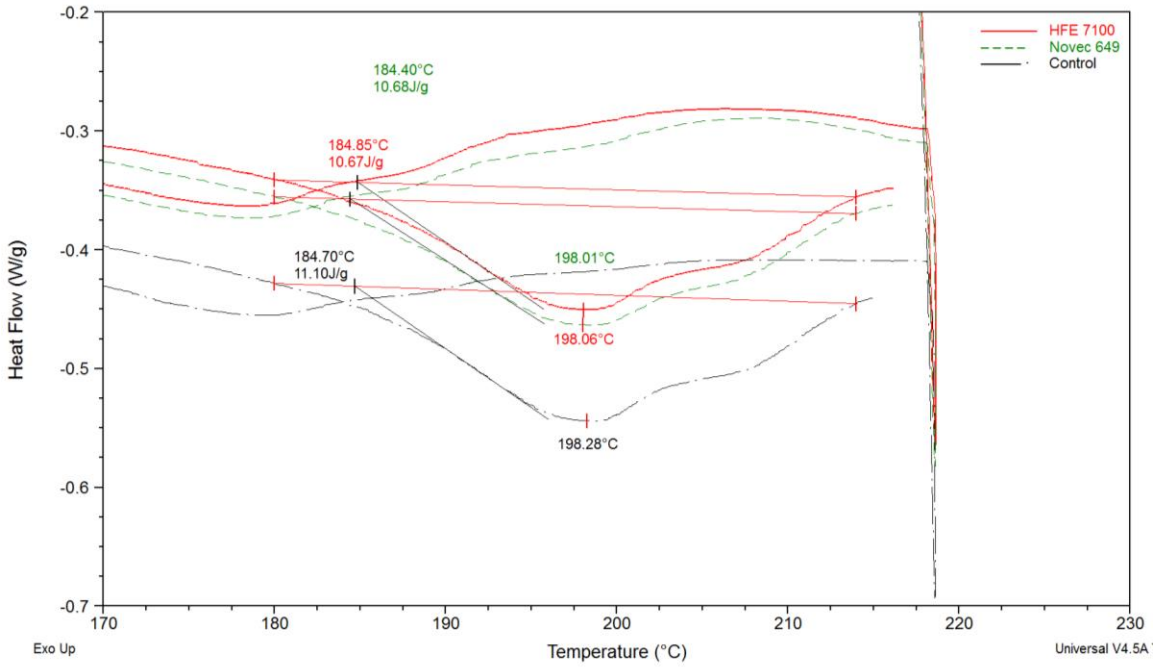

Figure 31. Linear integration of (29-1) polyurethane melting peaks after extraction with Novec 649 and HFE-7100.

Figure 32 shows the thermal degradation profile of a piece of (21) PVC tubing after extraction with Novec 649 in comparison to that of a control. Examining the temperatures at which 95% of the mass was lost does not reveal a significant change for the extracted sample nor does a comparison of the total mass lost at 550°C. Similar results were found for the (29-1) polyurethane tubing samples. Figure 33 displays a sectioned DSC thermogram of a (24) Nalgene sample after extraction with all three fluids in comparison to a non-extracted control. Nalgene is a proprietary polymer blend that contains low density polyethylene, a semi-crystalline polymer. Some changes in the melting temperature around -42°C and crystallization peak around -70°C were observed, however, further research would need to be conducted to understand the significance and reproducibility of these results.

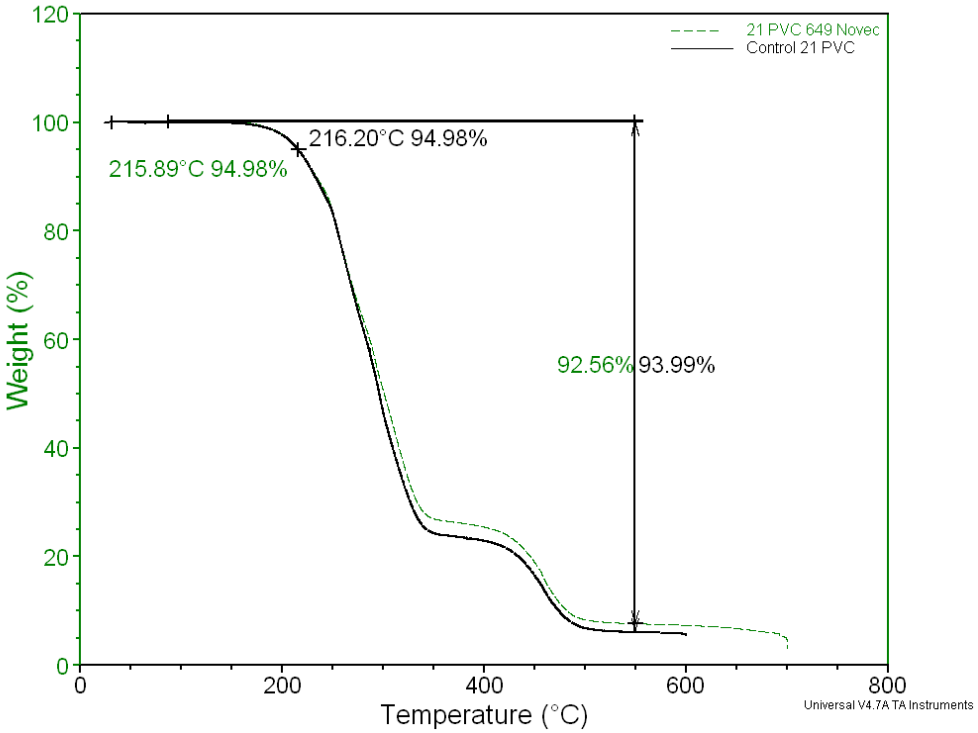

Figure 32. Thermal degradation of (21) PVC after extraction with Novec 649.

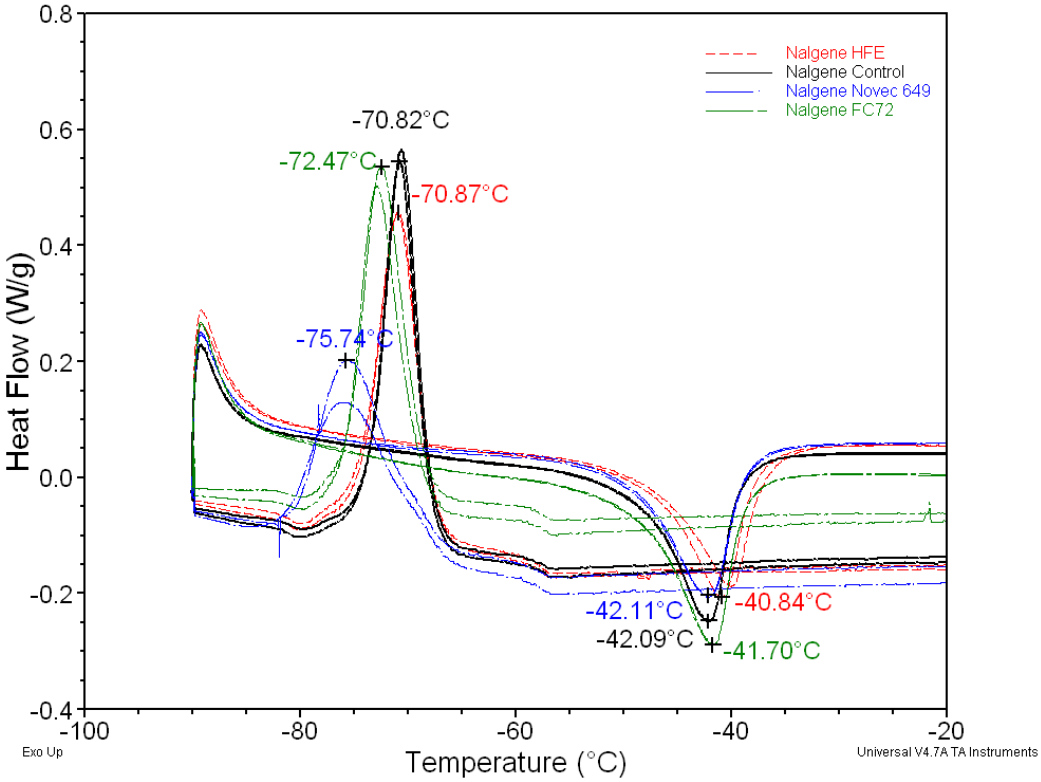

Figure 33. DSC of (24) Nalgene after extraction with all three dielectric fluids.

Material degradation due to loss of plasticizers and other additives is less likely to be a concern for immersion cooled HPC applications than applications where the components are subjected to repeated spooling, bending or other handling; however, it is possible that the changes noted above could result in a reduced life cycle. Additional research focused on the materials and not the fluid would be needed to better evaluate this potential issue. In the interim, the results above suggest that not only are materials with low extractables less likely to impact fluid performance, they are less likely to deteriorate.

4.1.5 Identification of Contaminants

A combination of attenuated total reflectance Fourier transform infrared (ATR-FTIR) spectroscopy, ultraviolet-visible spectroscopy (UV-Vis), and gas chromatography mass spectrometry (GC/MS) were used to aid in identifying contaminants within component residues. These methods were not intended to yield relative concentrations of contaminants, but to identify the materials comprising the total mass extracted determined in the mass balance. Although it is difficult to completely determine an unknown composition with ATR-FTIR, background knowledge of the polymers and their typical additives were used to determine the legitimacy of the suggested match results. When possible, literature searches were used to specifically identify the primary chemical compounds for ATR-FTIR spectra. However, in many cases extraction of multiple components and small residual (sample) amounts made it difficult to acquire confidence in the species matched.

Upon analysis of component residues, consistent match results were returned for polymer additives - primarily plasticizers. Table 8 provides a representative list of species matches to the contaminants found within the (21) PVC tubing residue after extraction with Novec 649. The main contaminant detected was bis(2-ethylhexyl) phthalate, also known as dioctyl phthalate (DOP). Three libraries confirmed its presence along with the greatest probability match percent of 88.08%. Dibutyl, dioctyl, and diheptal phthalate, different molecular weight analogs of the same material, were also found.

Table 8. ATR-FTIR match results for (21) PVC tubing residue after extraction with Novec 649.

Match	Compound name	Library
88.08	Bis(2-ethylhexyl) phthalate	HR Specta IR Demo
84.71	Tygon polymer R-1000	HR Nicolet Sampler Library
82.50	Dioctyl phthalate	HR Nicolet Sampler Library
82.50	Dioctyl phthalate	HR Nicolet Sampler Library
82.50	Dioctyl phthalate, 99%	HR Aldrich Esters, Lactones, and Anhydrides
81.81	Tygon polymer B-44-4X	HR Nicolet Sampler Library
79.31	Diheptyl phthalate, 97%	HR Aldrich Esters, Lactones, and Anhydrides
78.58	Dibutyl phthalate	HR Specta IR Demo
78.56	Hexanal, 98%	HR Aldrich Aldehydes and Ketones
77.67	Alkyd resin	Hummel Polymer Sample Library

Analyzing the residues of the individual components subjected to accelerated testing via ATR-FTIR led to the creation of a list of probable contaminants expected to leach from each component material. This list was useful in determining the source of unknown contaminants such as those from the small scale tank testing. Initial analysis of the Novec 649 and HFE-7100 tank test samples consistently returned high match percentages to nonyl aldehyde via ATR-FTIR. In comparing this result with the list of ATR-FTIR match data accumulated from accelerated testing, this contaminant was linked to (0-3) PVC ribbon and (40) PVC wiring insulation. Samples of (0-3) PVC ribbon and (40) PVC wiring insulation were again tested in all three fluids to develop confidence in the initial Soxhlet extraction match data. (0-3) PVC ribbon showed a match to nonyl aldehyde as well as trihexyl trimellitate, found to be another plasticizer.

In an effort to determine other potential sources of contaminant present within the tank testing samples, attention was focused on the containers used for fluid transport and storage – specifically the lining. Samples were collected from an FC-72 fluid container of

the opaque high density polyethylene (HDPE) cap/pour neck and the white Tri Sure seal covering the cap (found on fluid drums), shown in Figure 34. The HDPE cap was extracted with all three fluids and the Tri Sure seal was extracted with HFE-7100. Initially, ATR-FTIR was attempted on the fluid samples collected. Due to the small amount of contaminants present, ATR-FTIR did not register any peaks. To compensate, all samples were allowed to evaporate and the remaining residues were analyzed. The HDPE cap ATR-FTIR match results showed the greatest comparison to hexadecane in all three fluids. The Tri Sure seal showed matches to nonyl aldehyde and bis(2-ethylhexyl) phthalate (DOP). ATR-FTIR match results are provided in Table 9. Given these findings and after discussions with the tank testing personnel, it is possible that the Tri Sure seal came into contact with the tank test fluids. The nonyl aldehyde match shown from the ATR-FTIR analysis of the tank test samples could have been the result of this contact or inadvertent PVC contamination.

Although comparison of the results from the tank testing residues with the compiled list of probable contaminants yielded a positive identification, it was determined that the limits of ATR-FTIR (e.g., multiple contaminants present in the sample) might have not have provided an accurate representation of all of the contaminant species present within samples - both accelerated testing extraction residues and tank testing. ATR-FTIR worked well to confirm trends and match contaminants that were expected to show after Soxhlet extraction of a component material but an additional method was ultimately needed for identification of the range of contaminants within the tank test samples. Gas chromatography-mass spectrometry (GC/MS) was chosen for its ability to separate out multiple contaminants as well as its potential to identify the individual species.

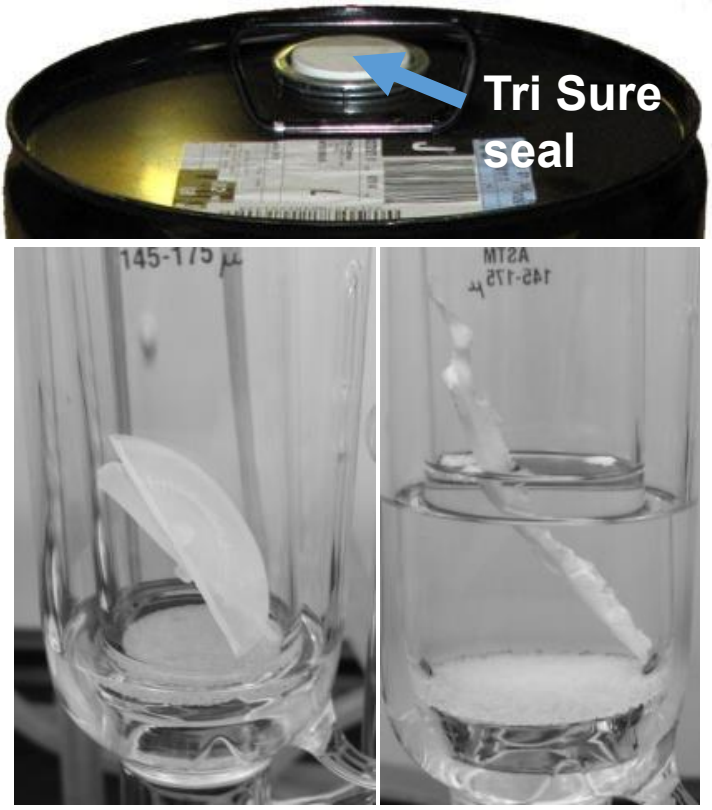

Figure 34. HDPE cap/pour neck (left) and Tri Sure seal (right).

Table 9. ATR-FTIR match results for Tri Sure seal.

Match	Compound name	Library
83.77	Nonyl aldehyde, 98%	Aldrich Condensed Phase Sample Library
81.11	Nonyl aldehyde, 95%	HR Aldrich Aldehydes and Ketones
80.48	Decyl aldehyde, 95%	HR Aldrich Aldehydes and Ketones
80.18	Dodecyl aldehyde, 92%	HR Aldrich Aldehydes and Ketones
78.66	Bis(2-ethylhexyl) phthalate	HR Specta IR Demo
77.52	Alkyd resin	Hummel Polymer Sample Library
77.28	Undecyclic aldehyde, 97%	HR Aldrich Aldehydes and Ketones
77.17	Tygon polymer R-1000	HR Nicolet Sampler Library
76.60	Tridecanal, Tech., 90%	HR Aldrich Aldehydes and Ketones
75.50	Octyl aldehyde, 99%	HR Aldrich Aldehydes and Ketones

Initially, a concentrated HFE-7100 fluid sample that went through nineteen data runs within the test tank was analyzed with GC/MS. This sample was produced by

allowing the HFE-7100 fluid to evaporate, leaving behind the contaminant residue. This residue was dissolved within acetonitrile for injection. The spectrum yielded for this sample can be seen in Figure 35. The spectrum clearly exhibits multiple peaks, indicative of several compounds present. Analysis of the individual peaks with comparison to the NIST/NIH/EPA Mass Spectral Library allowed for determination of the individual components present. Table 10 provides these results along with the percent match provided by the spectral library. Figure 35 also shows the comparison of the spectrum of the sample at 24.73 minutes (red) with that of the spectrum known for DOP (blue).

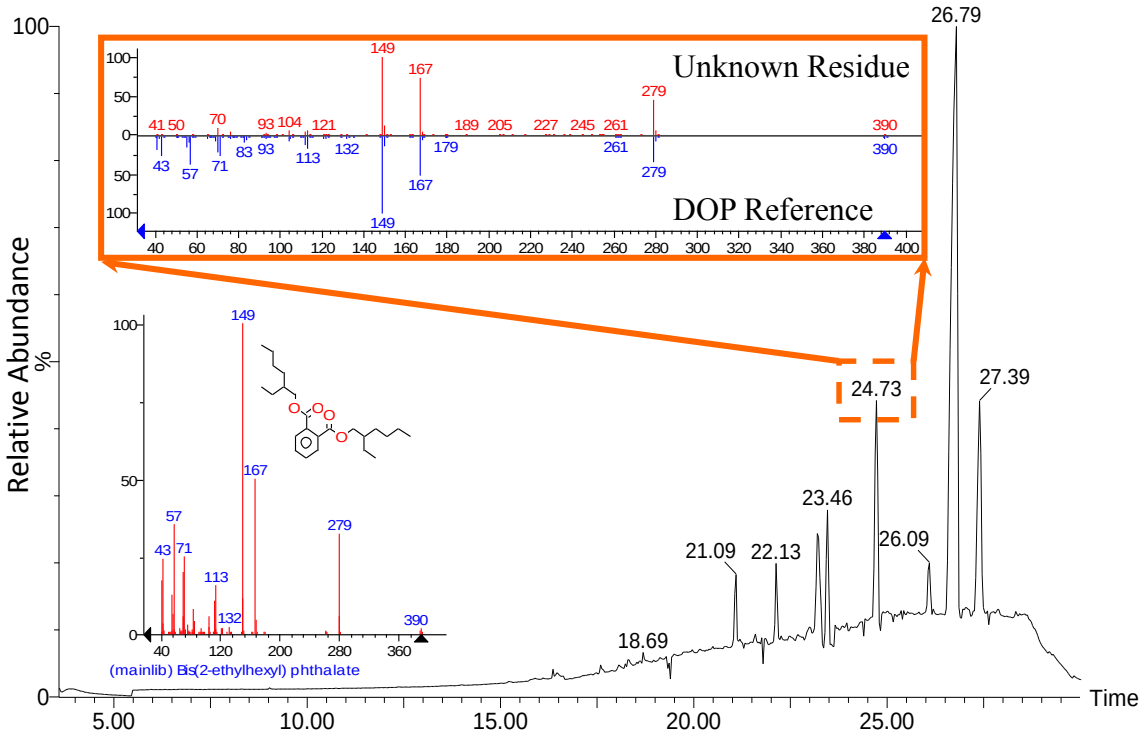

Figure 35. GC/MS spectrum of HFE-7100 sample after 19 data runs.

Table 10. GC/MS identified compounds from an HFE-7100 sample after 9 tank test thermal data runs.

Time	Identified Compound	Match %
18.69	9,10-Anthracenedione, dioxoanthracene	58.5
21.09	Phthalic acid, methyl neopentyl ester	48.0
22.13	Tributyl acetylcitrate	97.8
23.19	(Z)-9-Octadecenoic acid butyl ester	19.7
23.46	Hexanedioic acid, bis(2-ethylhexyl) ester	58.6
24.73	Bis(2-ethylhexyl) phthalate, dioctyl phthalate	61.9
26.09	Nonanedioic acid, bis(2-ethylhexyl) ester	62.6
26.79	1,3-Benzenedicarboxylic acid, bis(2-ethylhexyl) ester	94.0
27.39	Hexanedioic acid, bis[2-(2-butoxyethoxy)ethyl] ester	97.5

GC/MS analysis of the other tank test samples collected was conducted and a comparison of the spectra showed consistent peaks independent of the fluid or amount of data runs completed. Figure 36 shows a comparison of all of the tank test samples analyzed. This result suggest that new contaminants were not introduced into the system after the first sample was collected and that the previous contaminants remained through serial testing.

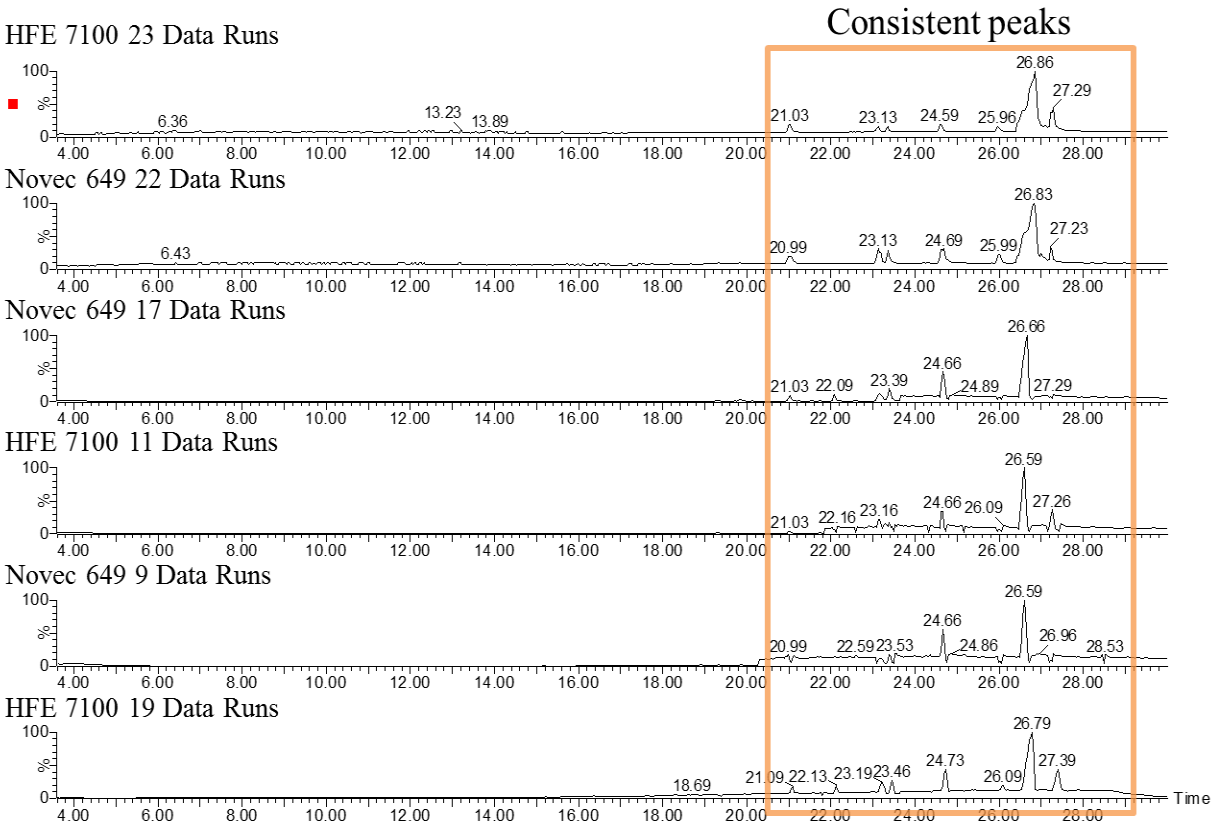

Figure 36. GC/MS spectra comparison of tank test samples.

4.1.6 Other Analysis Methods

Other analysis methods such as pH, optical microscopy, CRAIC, and scanning electron microscopy (SEM) were used to analyze the component materials and subsequent residues from accelerated testing as necessary. It was determined that the pH of the engineered fluids never changed (i.e., registered no pH) upon exposure to the component materials or after Soxhlet extraction, except in one isolated case. A pH change was registered after Novec 649 was exposed to water from the addition of activated carbon at atmospheric conditions and an acid was produced. The potential reaction of Novec 649 with water to form trifluoroacetic acid is a known potential issue with Novec 649. The acid produced after activated carbon addition resulted in the etching of some glassware.

Optical microscopy of the component materials before and after accelerated testing did not reveal any significant changes to the microstructure of the materials. This type of microscopy did prove useful in noticing the buildup of contaminant on the LTCC structures during powered testing. In most cases, particulates did not appear in the component residues except for within the residue of (25) natural rubber tubing after extraction with Novec 649 and HFE-7100. Figure 37 shows the comparison of the two particulate formations found. Within Novec 649, the solid contaminant appeared rod like and within HFE-7100 it appeared granular.

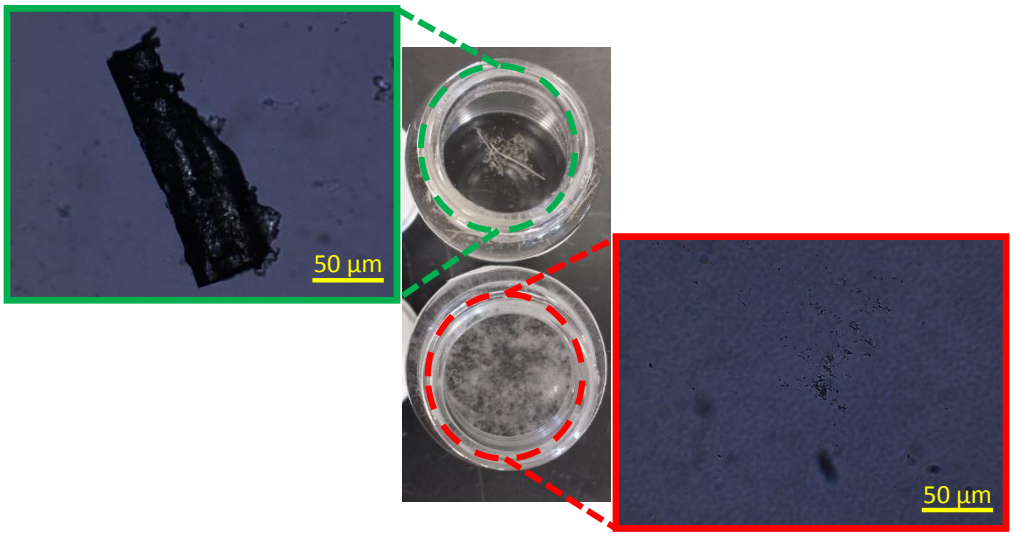

Figure 37. Residues from extraction of (25) natural rubber in Novec 649 (left) and HFE-7100 (right) and respective microscope images at 40x.

The use of the CRAIC UV-Vis-Fluorescent microscope was limited to the early investigation of residue structure elucidation. The instrument provided valuable insights, but was only capable of gathering data in transmission, so only transparent or translucent samples could be analyzed. The addition of an attachment to enable reflectance

measurements would make the instrument much more versatile as it would enable looking at deposits on the heat sinks, modules, and electrical contacts. Figure 38 shows the CRAIC UV-Vis spectra of the residue spots for (20) EPDM after extraction with Novec 649. It can be seen that analysis of multiple locations of the residue yielded a similar spectrum allowing for the conclusion that a singular contaminant or that of multiple similar contaminants were present. SEM was useful for examining the residues left behind on the LTCC structures after inclusion in the accelerated testing apparatus. Energy dispersive spectrometry (EDS) was used to analyze the chemical makeup of these residues (see 4.4 Combined Electrical and Thermal Compatibility Testing).

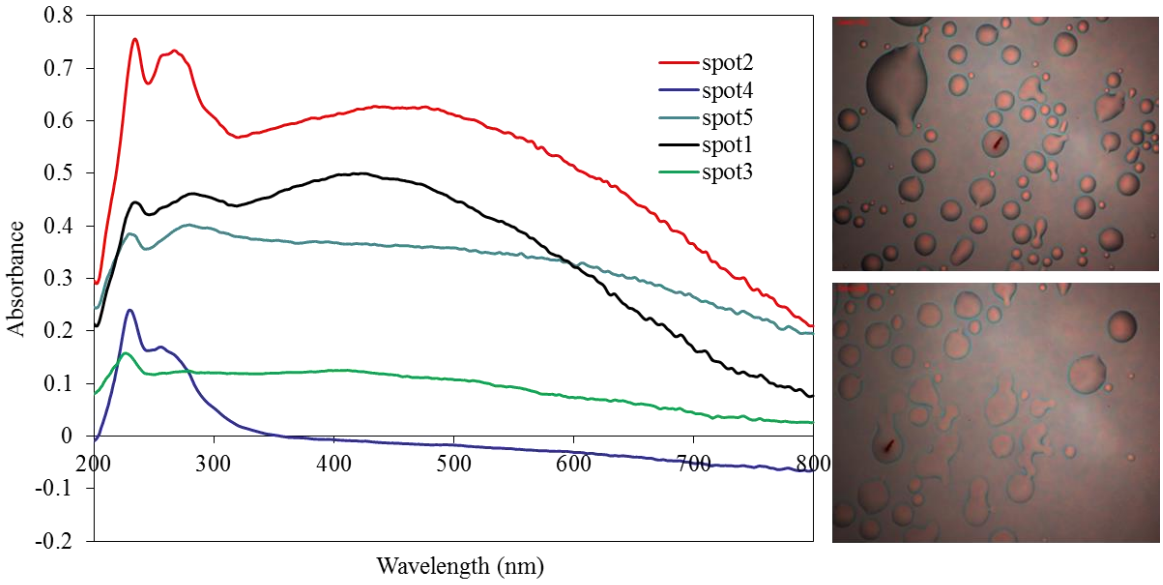

Figure 38. CRAIC UV-Vis spectra for a (20) EPDM residue after extraction with Novec 649.

The presence of multiple plasticizers within many materials prevented quantification. The residue from (42) chlorinated polyethylene wiring insulation showed similar condensing characteristics as that of (21) PVC tubing. Under the initial impression

that the contaminant was DOP, a sample was collected for UV-Vis analysis. The residue was analyzed via ATR-FTIR and determined to be a combination of DOP and bis(2-ethylhexyl) sebacate (DOS). The chemical structure of DOS, shown in Figure 39, does not contain two independent electronic characteristics like that of DOP (i.e., conjugated ring structure and non-bonding electrons). This meant the UV-Vis spectrum yielded only a single peak. Given that the residue from (42) chlorinated polyethylene wiring insulation contained both DOP and DOS, it was impossible to distinguish between the two without two peaks present in each species' individual spectrum. Two sets of peaks would have allowed the solving of a system of equations for arrival at the individual concentrations (i.e., two equations, two unknowns).

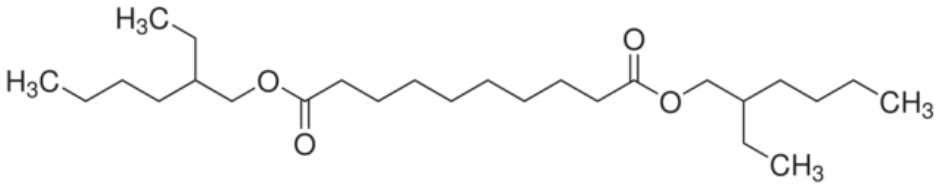

Figure 39. Chemical structure of bis(2-ethylhexyl) sebacate (DOS).

4.2 Laboratory Tests of Remediation Strategies

After subjecting the wide spectrum of proposed component materials to the accelerated testing procedure, it became clear that the most likely contaminants were plasticizers. The more pliable a material was, the more likely it was to leach contaminants into the solvent. Thus, it is recommended that soft polymeric materials be avoided when possible and more rigid structures chosen as replacements.

A remediation study was executed to determine the ability of removing additives such as plasticizers from the dielectric fluids. Dioctyl phthalate (DOP) was chosen as the model contaminant given its comprehensive use as a plasticizer. Activated carbon was chosen as the remediation media given its well-known uses in the consumer market and significant amount of surface area available for contaminant deposit. A Brunauer–Emmett–Teller (BET) analysis of the activated carbon yielded a specific surface area S_{BET} of 858.1 ± 20.5 m^2/g. SEM of the Fluval activated carbon shown in Figure 40 depicts the significant amount of surface area available for adsorption of organic contaminants. HFE-7100 was chosen as the initial solvent since 1) it has a KB value of 10 and 2) does not form an acid upon addition of water. Extending this method to Novec 649 would require careful drying of the carbon to make sure no moisture was introduced to the fluid.

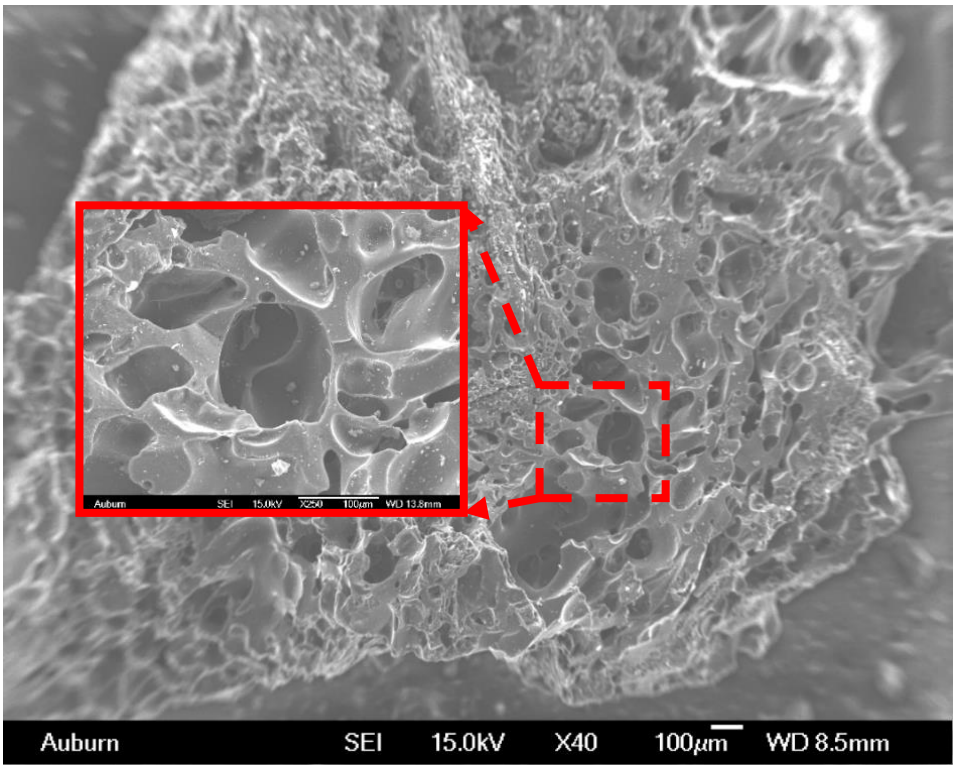

Figure 40. SEM image of Fluval activated carbon.

A stock solution of DOP and HFE-7100 was created. Equal amounts of the stock solution were distributed over varying masses of Fluval activated carbon. No consideration was given to the differences in the sizes of the Fluval pieces – a potential source of error. A sample was taken after twenty-four hours and the concentration of DOP determined via solvation in hexane and examination via UV-Vis spectrometry. No agitation was provided to the Fluval/HFE-7100/DOP vials except before sample collection. A slight swirling was applied to the vials to help ensure a representative sample was collected.

As shown in Figure 41, the addition of the carbon resulted in a decrease in the fluid's DOP concentration. The connecting lines are provided to guide the reader's eye. Standard error bars are shown for both concentration and Fluval mass. This shows that the carbon adsorbed the DOP as expected. Increased Fluval mass led to a decrease in DOP concentration. The greatest source of error within this experiment was from the rapid evaporation of the solvents used (i.e., HFE-7100 and hexane).

Given the apparent dependence DOP concentration has with time in the presence of Fluval, it was decided to examine the concentration change of a DOP/HFE-7100 solution after addition to a constant Fluval mass. 110 mL of a 0.231 g/L stock solution was added to a constant 1 g of Fluval. 1 mL samples were taken every five minutes for the first two hours and then at hour and day intervals thereafter. Figure 42 shows the data collected. The final concentration determined, after four days of exposure, is not shown. The concentration at this point was determined to be 0 g/L. The data is somewhat noisy. It is believed that the high point at 20 minutes is from a contaminated (i.e., previously used) cuvette, however, the other deviations are not readily explainable.

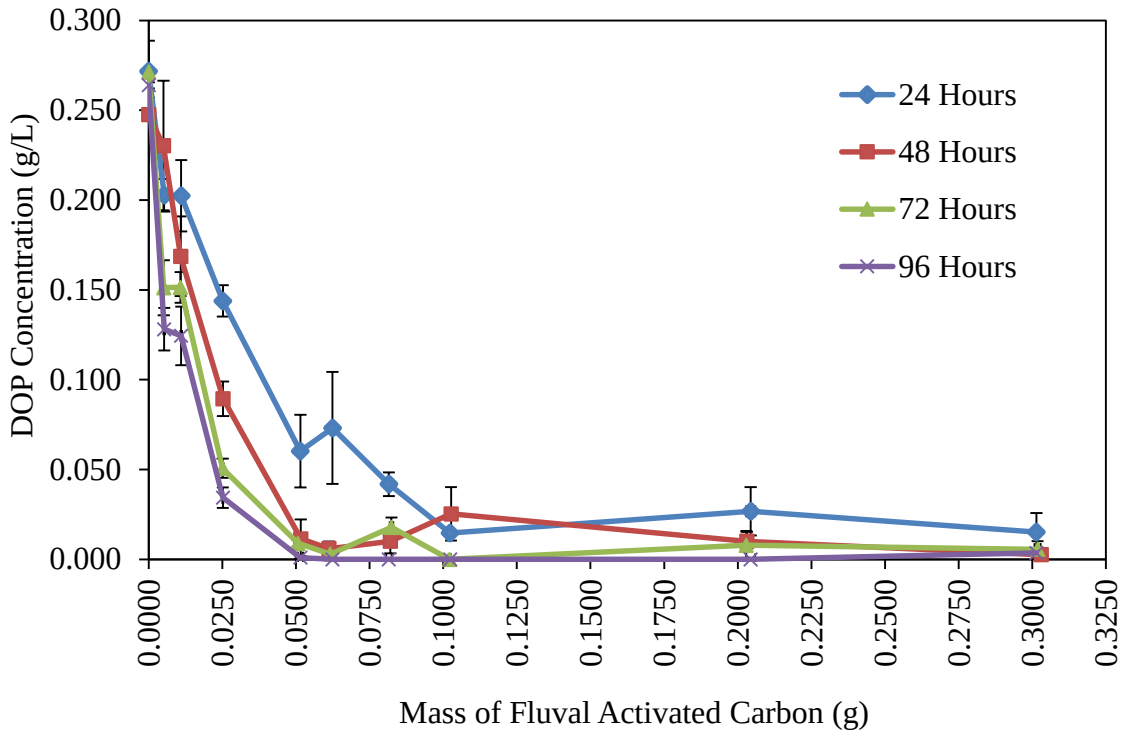

Figure 41. DOP concentration change via increasing adsorption onto activated carbon.

It is possible that during collection, samples were not taken from the same height within the vial and thus concentration determination could have been affected by a developed gradient within the experimental vial. In order to prevent this type of gradient forming, a slight swirl was applied to the solution before collection. The data roughly follows a linear trend (R^2 = 0.84), but repeated experiments would need to be completed to confirm and better quantify this relationship.

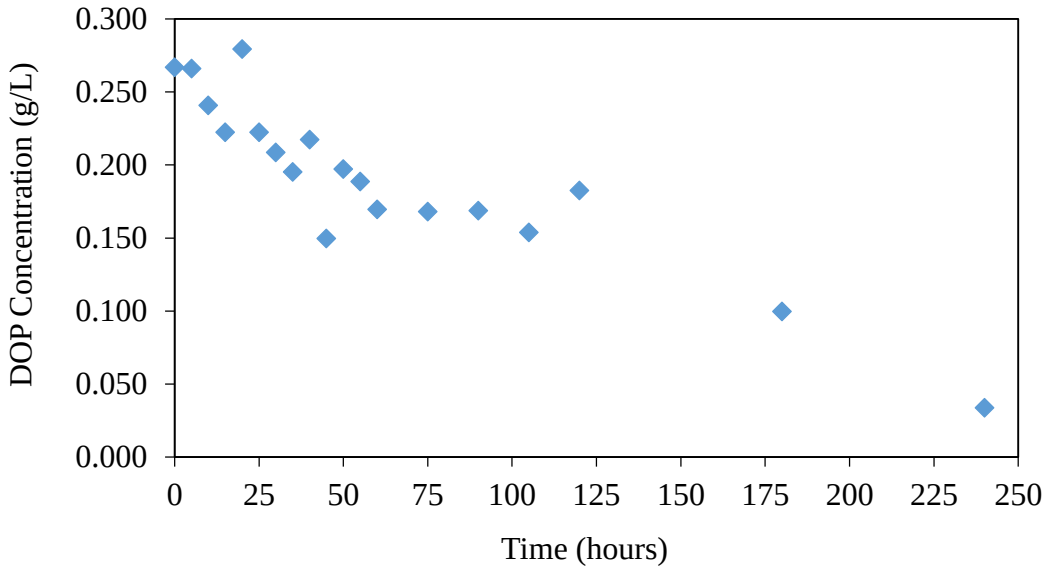

Figure 42. DOP concentration change with time given a constant mass of Fluval.

Given that phthalate plasticizers are similar in structure to one another, and carbon can adsorb a broad range of organic compounds, it is reasonable to assume this technique would be applicable in most cases where additive leaching occurs from polymeric components. In addition to the phthalate plasticizer studied, Fluval activated carbon was added to a bright yellow residue collected from (44) EPDM rubber tubing (see 4.1.3 Fluid Comparison) believed to be identified as thermoplastic elastomer (ATR-FTIR). After twenty-four hours of exposure, the sample residue cleared up and the ATR-FTIR results no longer showed the inclusion of thermoplastic elastomer in its match listings. Figure 43 shows the comparison of the sample residues before and after Fluval exposure.

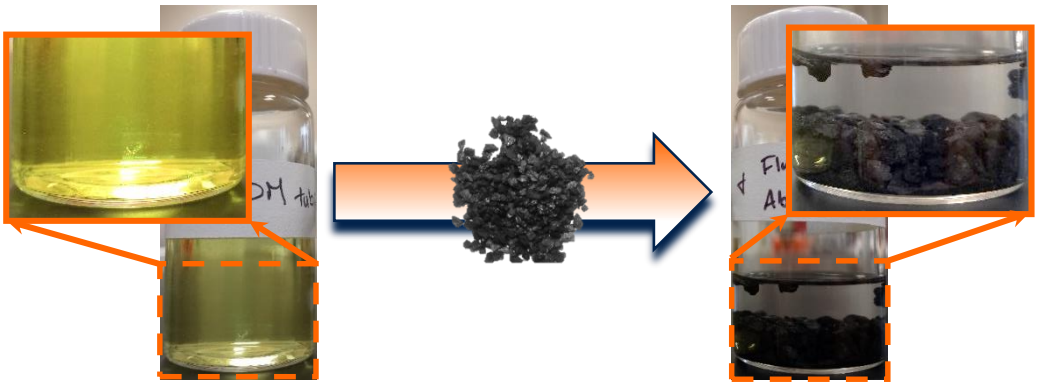

Figure 43. (44) EPDM rubber tubing residue before and after twenty-four hour exposure to Fluval activated carbon.

4.3 Thermodynamic Relationships

The experimental results of this research, growing awareness of the plethora of materials that could be used in immersion cooled HPC systems, and the differences in composition and extractability for seemingly similar materials such as EPDM highlight the need for choosing materials based on more than empirical results. Thermodynamic solubility of the additives in the polymers and in the fluids dictates the level of extractability that can be expected. The Kauri Butanol value has been used by 3M personnel as an indication of dielectric fluid solvent power [7]. However, the empirical basis of the KB value makes its applicability to dielectric fluids for immersion cooling questionable. Also, the data presented here highlights a discrepancy in the KB values of Novec 649 and FC-72. Both Novec 649 and FC-72 have been assigned KB values of zero but the data has shown in a number of cases the fluids extracted different amounts of materials from polymeric components. This further highlights the limited applicability of the KB value for this application. It would seem reasonable to refer to a solubility

parameter more widely studied such as the Hildebrand parameter or Hansen solubility parameters (HSP).

The widespread use of Hildebrand and HSP makes their identification for component species easily determinable via literature searches. Table 4 lists the KB and HSP values for several species encountered during accelerated testing. Following the general rule of "like dissolves like", those species with the most similar HSP would be most miscible. The values for the engineered fluids were predicted via several group contribution methods including the ThermoData Engine found in the ASPEN Plus software suite and the HSP group contribution method. The HSP group contribution method assumed first-order contributions. Two schemes were implemented for the molecular breakdown of HFE-7100. The first separated the methoxy group into its component oxygen and methyl groups and the second utilized them grouped. The two schemes used are illustrated in Figure 44 and the predicted solubility parameters are shown in Table 11. Surprisingly, this method did result in significant differences in HSP. Additional research using higher order interaction terms could provide new insights. Obtaining a more meaningful thermodynamic analysis that results in agreement between theory and observation would enable more rational material selection and provide information on specific preferred (or to be avoided) additives.

Table 11. Solubility parameters [27-29, 39].

Type	Species	Solubility Parameter	
		KB Value	Hansen $(MPa)^{1/2}$
Engineered Fluids	Novec 649	0	12.53
	HFE-7100	10	13.67
	FC-72	0	12.52
Plasticizers	Diethyl phthalate		20.55
	Dioctyl phthalate (DOP)		19.21
	Di-n-butyl phthalate		20.19
	Dioctyl sebacate (DOS)		17.47
	Dibutyl sebacate		15.17
	Triisooctyl Trimellitate		17.83
Polymers	Poly(vinyl chloride)	60	19.55
	Polypropylene		18.10
	Polyethylene (linear)		16.26
	Poly(methyl methacrylate)		21.52
Solvents	n-Hexane	29-30	14.90
	Acetonitrile		24.42
	Water	6.5	47.82

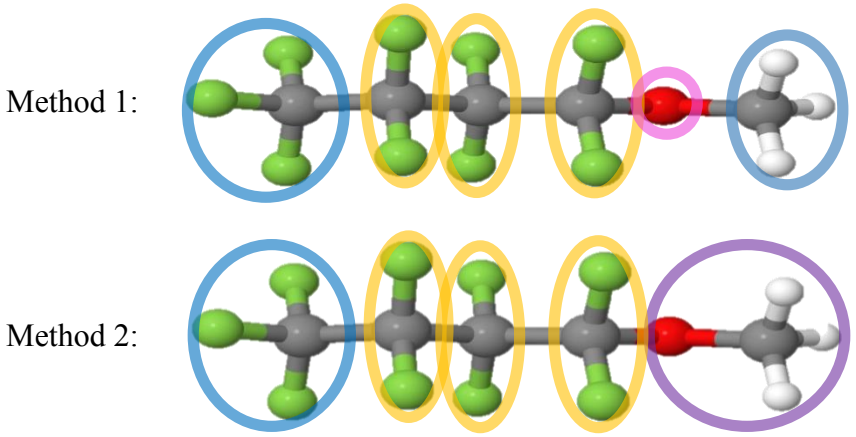

Figure 44. Group contribution breakdown of the two methods used for HFE-7100 HSP calculation.

Table 12. HSP via group contribution and ASPEN Plus prediction.

Fluid	Group Contribution $(MPa)^{0.5}$	Aspen Predicted $(MPa)^{0.5}$	% Difference
Novec 649	20.07	12.53	60.3%
HFE-7100 (1)	12.33	13.67	9.9%
HFE-7100 (2)	12.05		11.9%
FC-72	8.31	12.52	33.6%

4.4 Combined Electrical and Thermal Compatibility Testing

Given the presence of electric fields within immersion cooling applications, an attempt was made to examine the effect its presence may have on the interaction of component materials and the dielectric fluids. A 5 V direct current (DC) was applied to a DuPont 9K7 LTCC and Si substrate with Asahi AL-X thin films forming various distances of open structures (0.125, 0.5, and 1.0 mm). Figure 45 shows a representative structure used during testing. Testing was completed in all three fluids with several component materials under extraction: (18) Tygon tubing, (21) PVC tubing, (24) Nalgene tubing, (20) EPDM, (25) natural rubber, and (39) Teflon wiring insulation. These materials, except Teflon, were chosen due to their previously well characterized ability to leach contaminants during accelerated testing. Testing was completed with the powered structures located within the extractor thimble and within the round bottom flask.

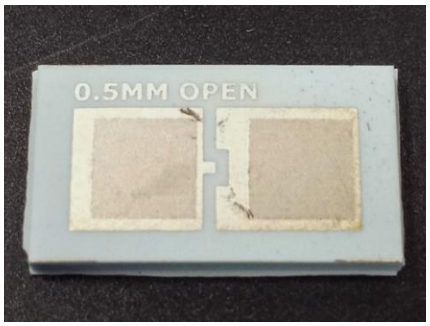

Figure 45. Gap structure used in powered Soxhlet testing.

4.4.1 Powered Structures in Soxhlet Thimbles

A powered, open gap structure was placed alongside the component material within the Soxhlet thimble. Initially, several gap sizes were explored to look for potential effects the leachable species may have on the powered structures. Figure 46 shows a typical placement of the gap within the Soxhlet apparatus.

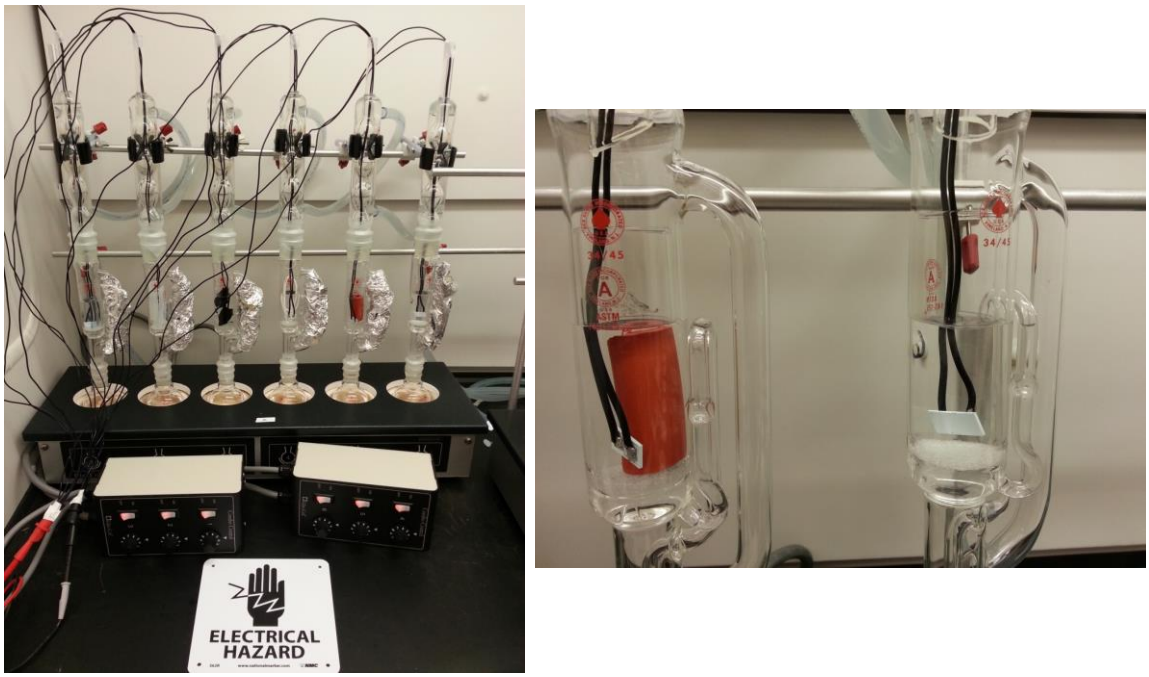

Figure 46. Powered gap structures placed within thimble of Soxhlet extractors next to component materials during accelerated testing.

After initial extraction of the component materials in the presence of a powered gap structure, discoloration and possible deposition was noticed on a few of the gaps placed within the thimbles. In order to determine the source of this buildup and whether or not it was a concern, the materials were gold coated and both SEM and EDS were performed. Example optical microcopy images are shown in Figure 47. SEM images and EDS spectra are shown in Figure 48 and Figure 49, respectively. The EDS results were not conclusive.

The detected silver was from the coating and the other elements could have come from the device itself or incidental contamination. In addition, DOP could have been the cause of the oxygen peak but oxygen is a very common contaminant in EDS measurements.

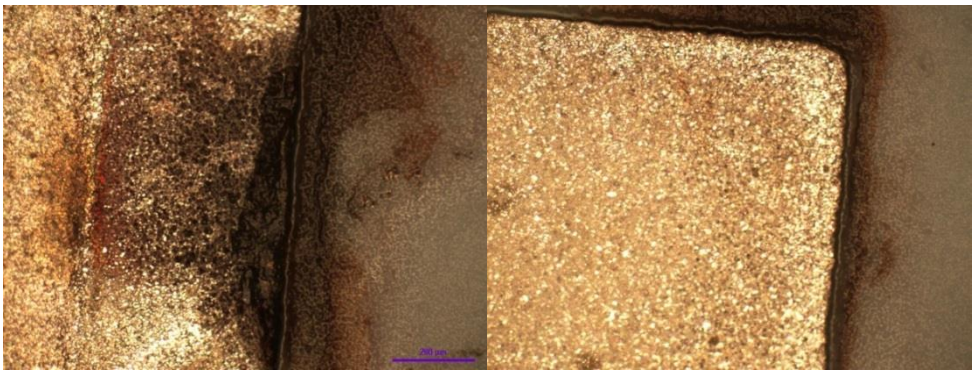

Soldered ceramic board from PVC-Novec 649 powered (10X)

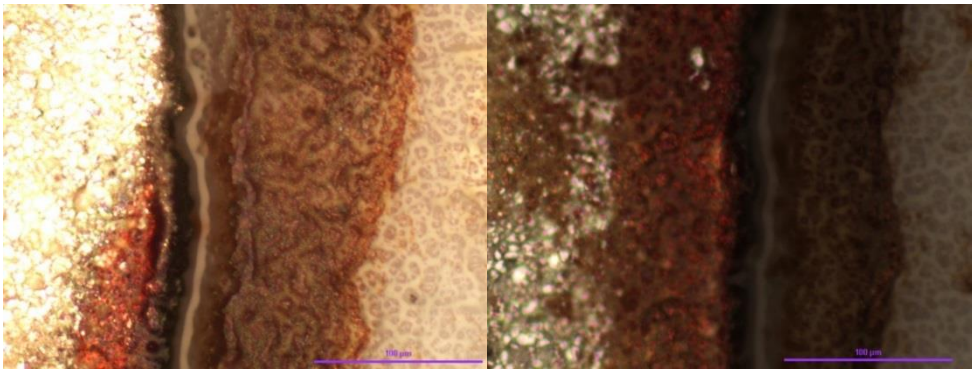

Soldered ceramic board from PVC-Novec 649 powered (40X)

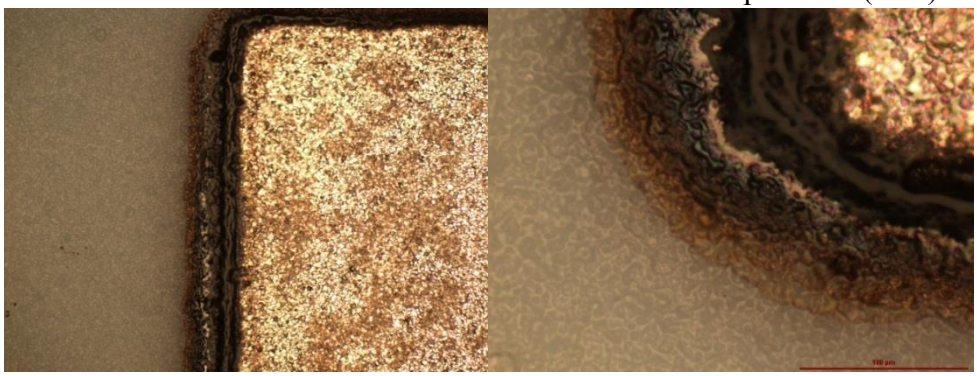

Soldered ceramic board from EPDM-Novec 649 powered (10X and 40X)

Figure 47. Optical microscopy images of powered gap structures after Soxhlet extraction of (21) PVC in Novec 649.

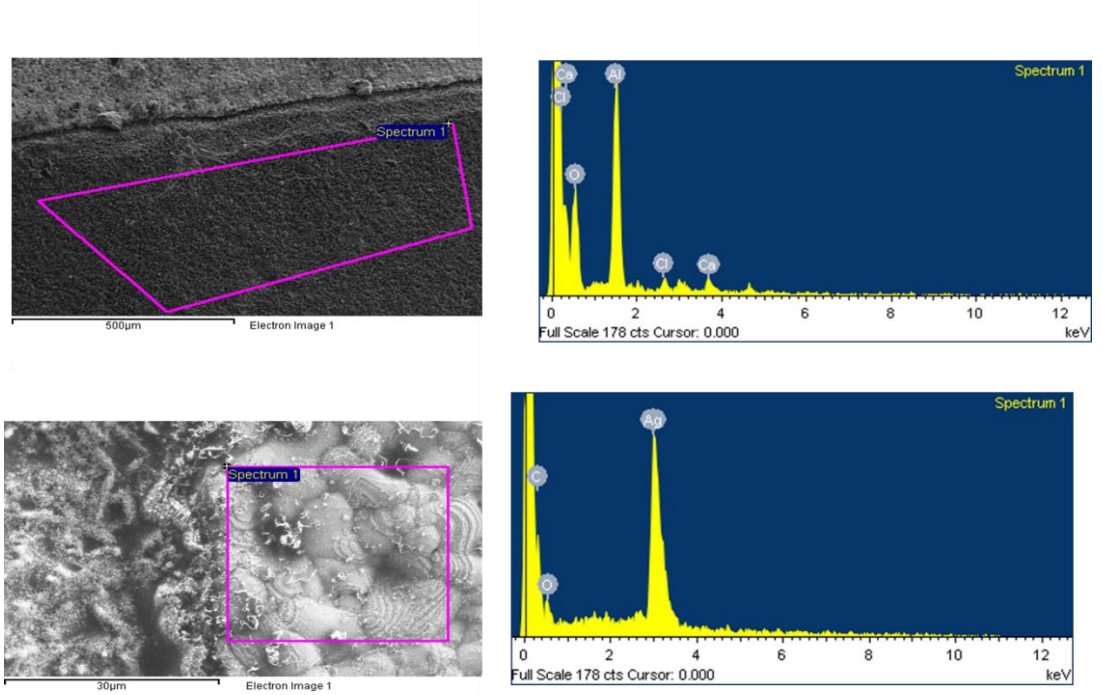

Figure 48. SEM and EDS data of gap structures after accelerated testing of (21) PVC tubing.

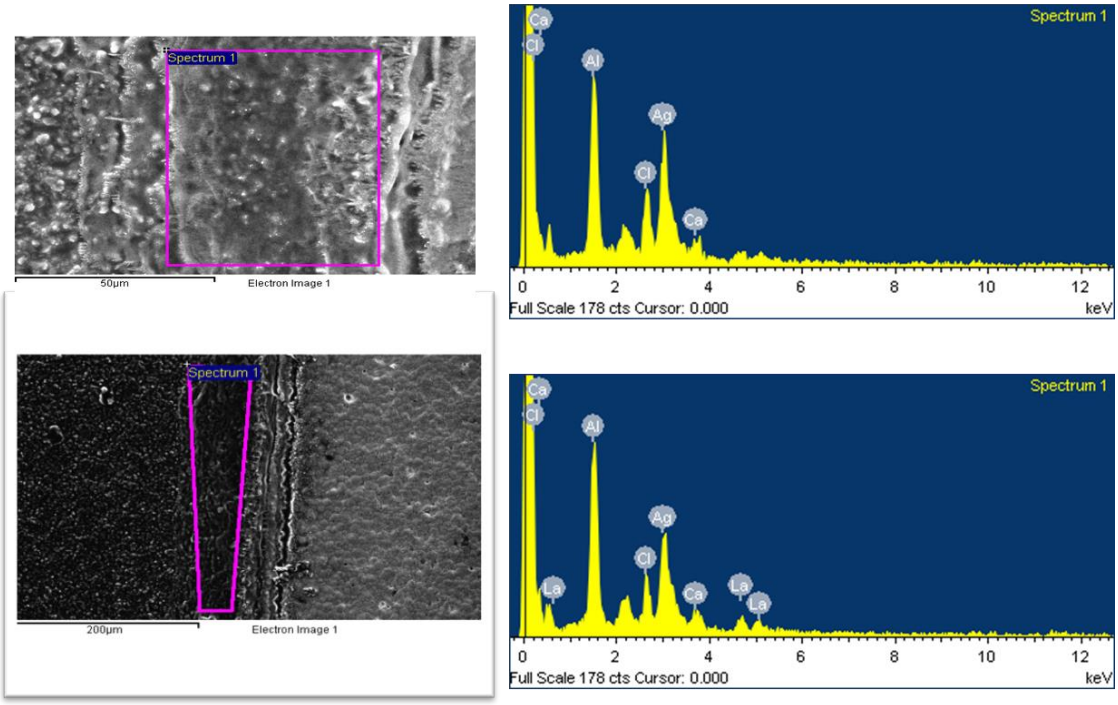

Figure 49. SEM and EDS data of gap structures after accelerated testing of (20) EPDM.

In addition to any effects observed on the gap structures themselves, mass balances were conducted on the component materials to look for changes compared to the standard Soxhlet extraction data. Figure 50 and Figure 51 show the mass extracted and mass absorbed figures for the varying gap sizes, respectively. Most of the masses extracted for the powered runs remained below their respective non-powered counterparts, but the data was not statistically significant due the lack of additional repeated experimental data and the variances of masses of (21) PVC tubing chosen for testing. However, given that all of the mass extracted data for (21) PVC was below 5.0% and the predicted maximum amount of plasticizer present was 36.4%, it is reasonable to conclude that the powered structures did not yield a result worth concern for adoption within cooling applications. The missing mass extracted data for (21) PVC tubing is a result of an experimental mishap. This instance was not repeated given the complexity of setup and expense of materials. The mass extracted data for (39) Teflon wiring insulation was 0.0%.

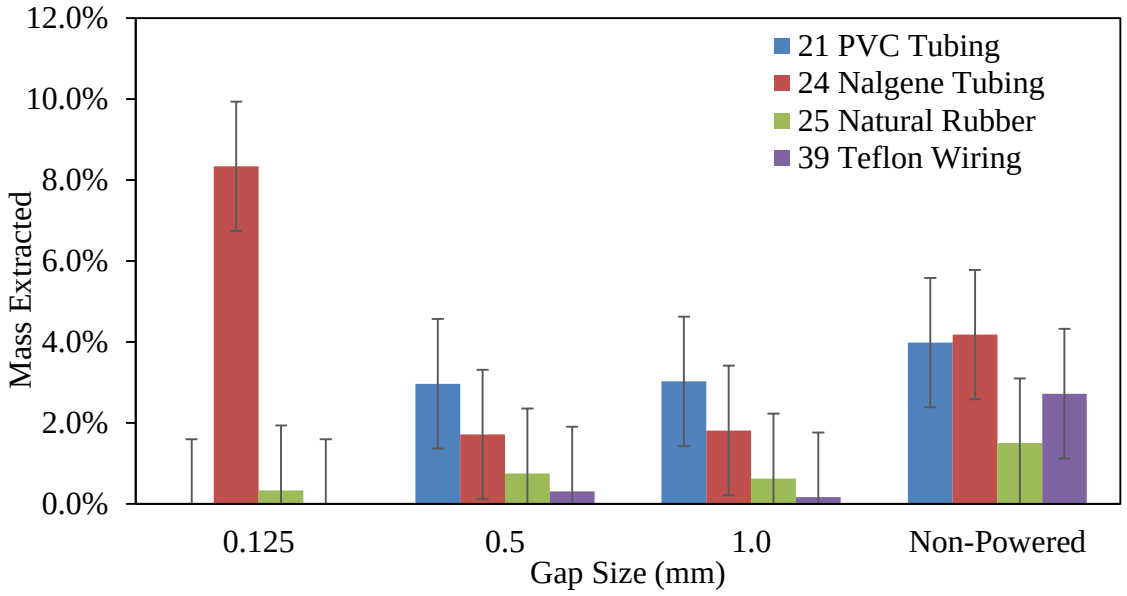

Figure 50. Mass extracted percentages for materials exposed to powered gap structures during extraction with Novec 649.

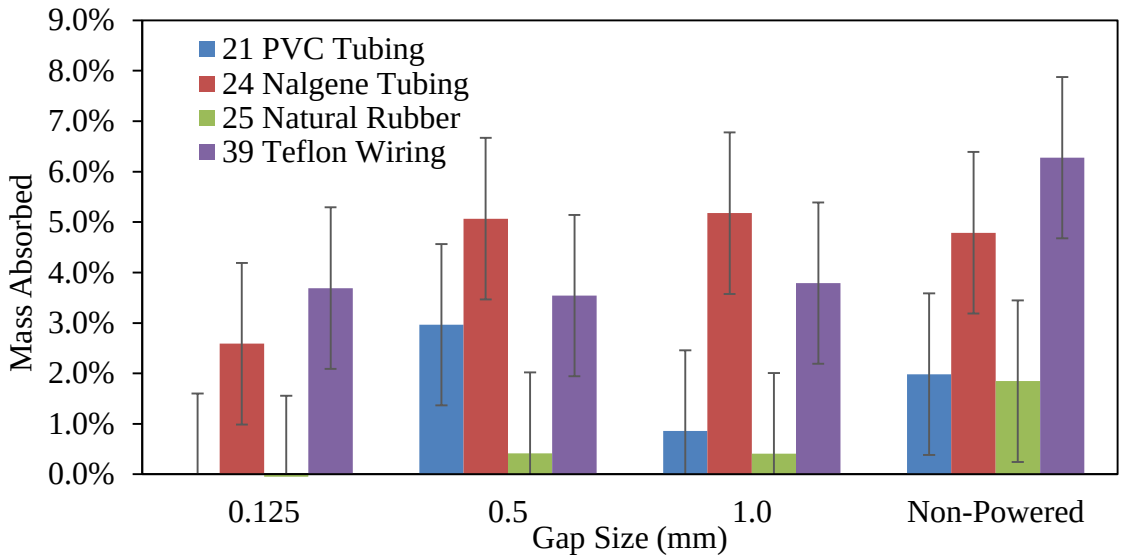

Figure 51. Mass absorbed percentages for materials exposed to powered gap structures during extraction with Novec 649.

After exploring the various gap sizes within Novec 649, a common size of 0.5 mm was settled upon for testing in the other two engineered fluids. At this width and applied voltage, a field of 10 kV/mm was created. A comparison of the masses extracted and absorbed for runs with a 0.5 mm gap present and without are provided in Figure 51 and Figure 52. Again, it is difficult to note specific trends in the data. The HFE-7100 mass extracted value for (39) Teflon wiring is believed to be the result of an experimental error given that the chemical structure similarities between Teflon and the fluids should result in swelling (absorption) rather than extraction. Most of the masses extracted for components in the presence of the gap structures are within error of the non-powered data. In addition, the masses extracted in all three fluids appear within error of each other for (21) PVC tubing, (24) Nalgene tubing, and (25) natural rubber leading to the conclusion that the powered structures had no obvious effect on the accelerated testing of the materials themselves.

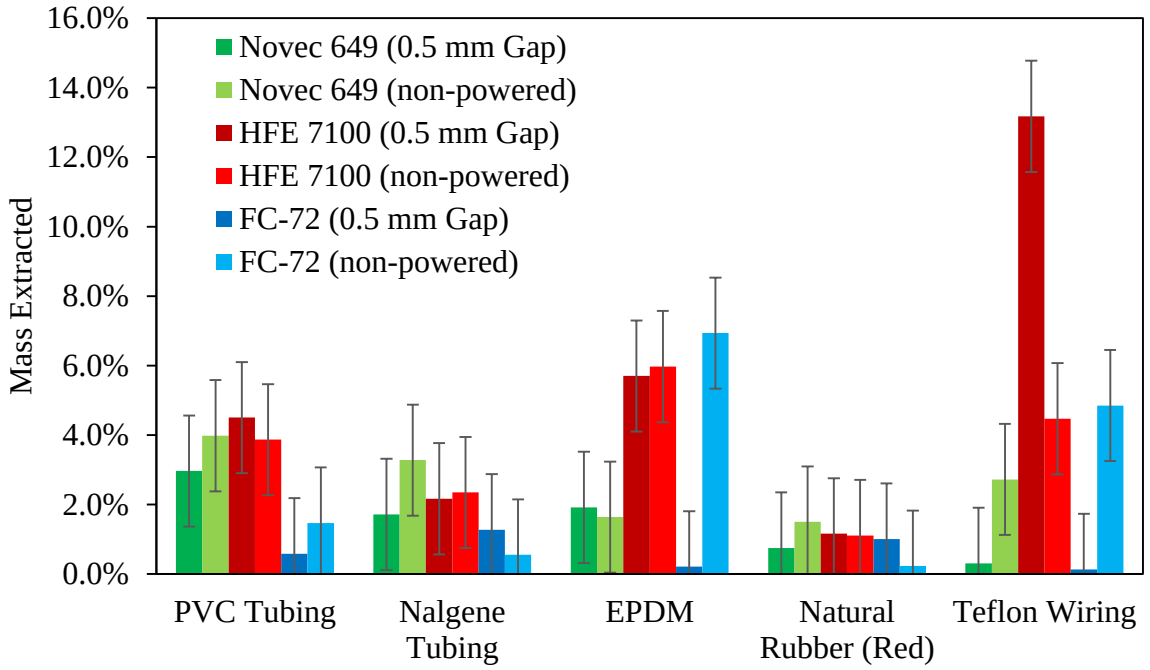

Figure 52. Materials extracted with Novec 649, HFE-7100, and FC-72 in the presence of a 5V powered 0.5 mm gap strucutre placed in the Soxhlet thimble.

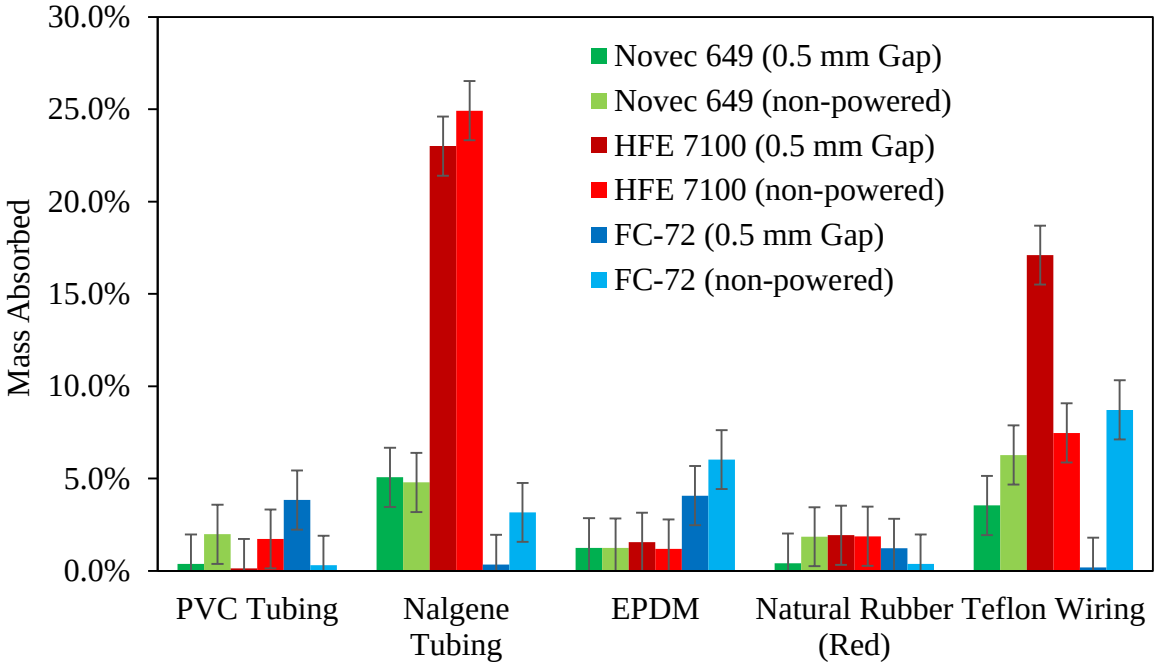

Figure 53. Materials extracted with Novec 649, HFE-7100, and FC-72 in the presence of a 5V powered 0.5 mm gap structures placed in the Soxhlet thimble.

4.4.2 Powered Structures in Round Bottom Flasks

It was determined during powered testing with gap placement inside of the extraction thimble that since only the distilled fluid reaches the thimble, the contaminants (i.e., leachable species) were not coming in contact with the gap structure itself. It was decided that placing the gap within the round bottom flask (RBF) may yield a more realistic simulation as the amount of contaminant built up during the extraction period. New glassware was designed for this purpose and the tests were rerun with all three dielectric fluids. Figure 54 shows the modified extraction setup.

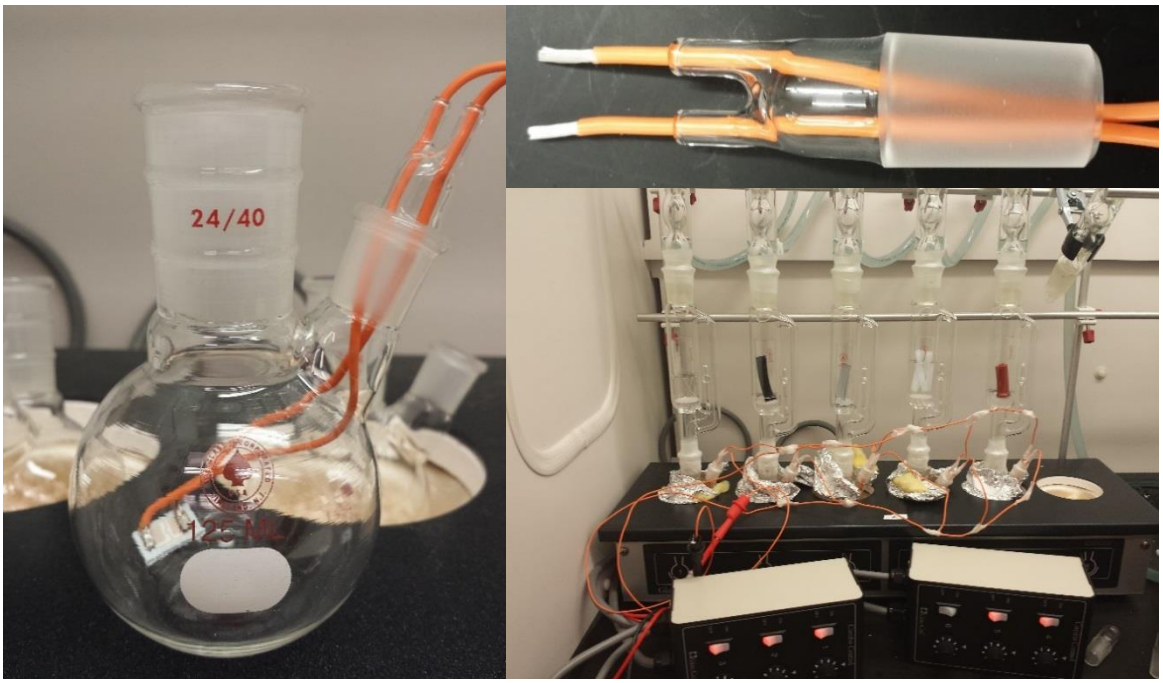

Figure 54. Powered gap structures placed within the round bottom flask of Soxhlet extractors during accelerated testing.

Even with the increase in contaminant concentration around the powered gap structures, completion of the circuit was not discovered in any of the runs. Mass balances did not show any unique results. Comparisons were made between the masses extracted

and absorbed where the powered structure was present in the thimble and when the structure was absent. Figure 55 and Figure 56 show these comparisons within HFE-7100. Again, most of the data falls within the estimation of error.

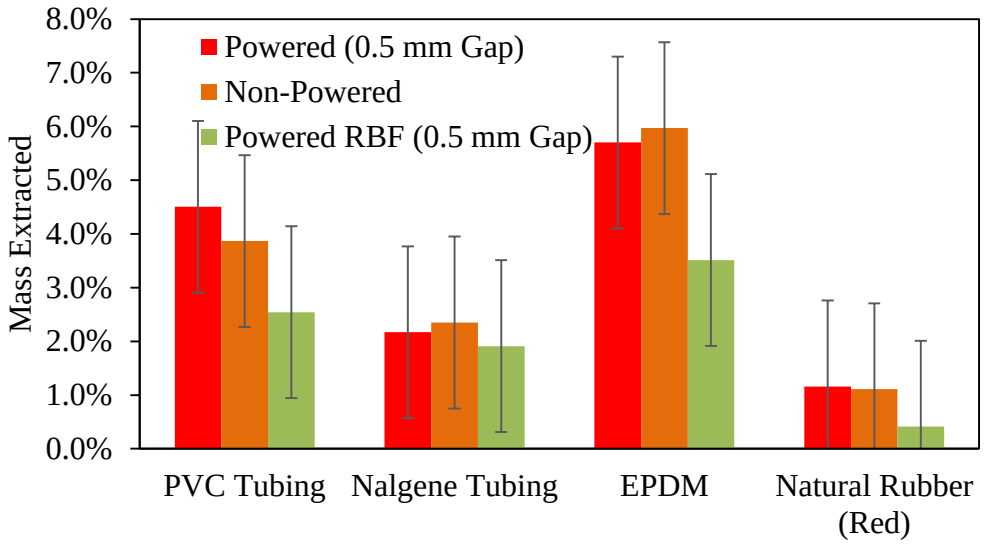

Figure 55. Mass extracted figures for materials extracted with HFE-7100 in the presence of a powered gap and without.

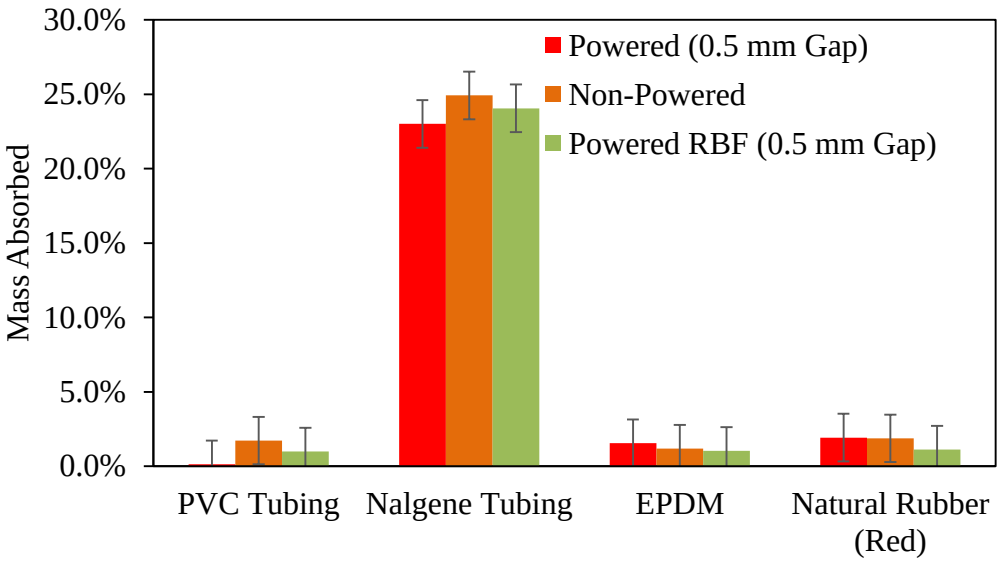

Figure 56. Mass extracted figures for materials extracted with HFE-7100 in the presence of a powered gap and without.

Microscope images were taken of the gap structures from the RBF powered runs. Buildup of contaminant on the gap structure was discovered as well as between the gap itself. Figure 57 shows the presence of DOP from a (18) Tygon sample after extraction with FC-72 and a (21) PVC sample after extraction with Novec 649. ATR-FTIR confirmed the presence of DOP on these structures. Similar results were observed for the gap structures from (20) EPDM after extraction with HFE-7100 and Novec 649, (21) PVC tubing after extraction with HFE-7100 and Novec 649, and (25) natural rubber after extraction with FC-72. Although residue was discovered on some of the structures, others were clean. Figure 58 shows the gap without contaminants for (24) Nalgene after extraction with FC-72 and an unused thru structure.

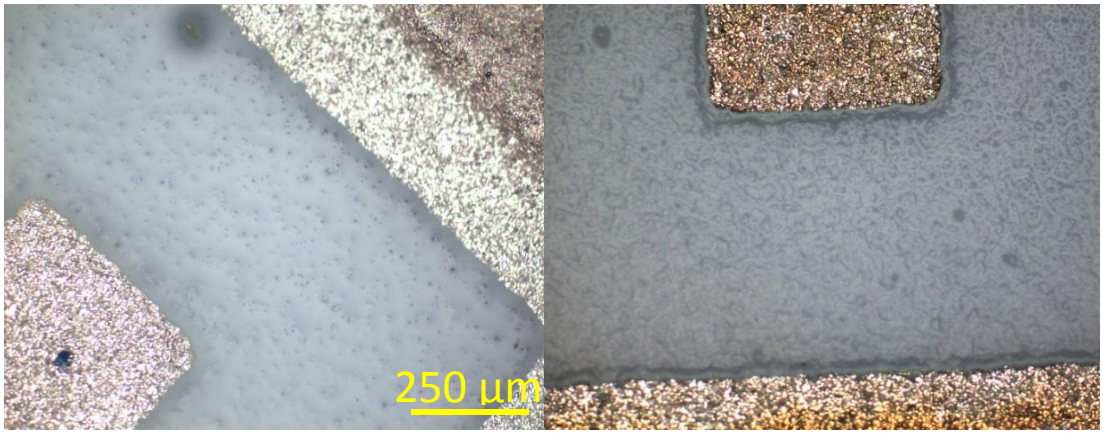

Figure 57. Gap structures at 20x after extraction within the round bottom flasks of (18) Tygon in FC72 (left) and (21) PVC in Novec 649.

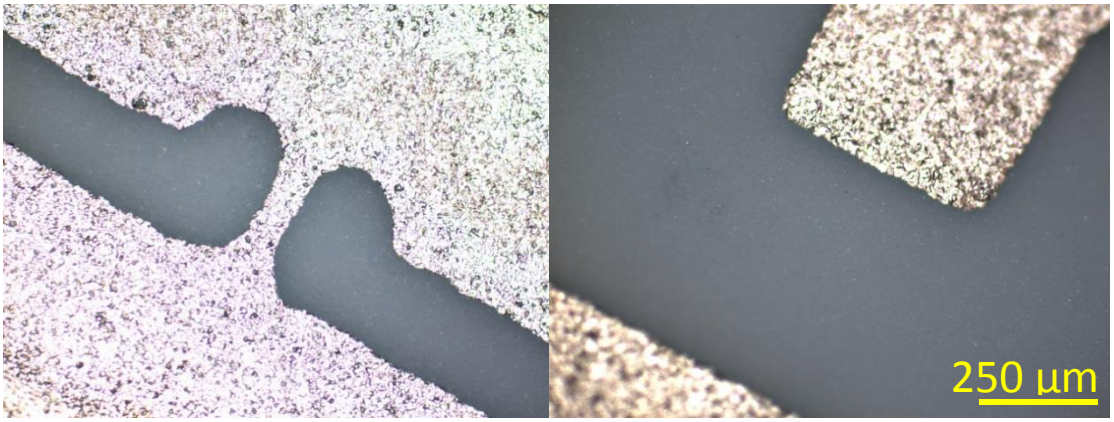

Figure 58. An unused thru structure (left) and (24) Nalgene after extraction with FC72 (right).

4.5 Small Scale Tank Testing Using Contaminated Dielectric Fluid

A small scale system test was conducted using Novec 649 after deliberate contamination with DOP. It was found that the provided tank test sample of HFE-7100 after nineteen data runs exhibited a total contaminant concentration of 0.161 g/L HFE or 0.011 wt% contaminants and a sample of Novec 649 after twenty-two data runs exhibited a contaminant concentration of 0.129 g/L or 0.008 wt% contaminants. The amount of DOP added to the dielectric fluid was estimated to about three times higher than the highest amount of contamination observed in Soxhlet extraction. This value was used to estimate a worst case scenario concentration, and 30 mL of DOP were added to 8L of Novec 649 yielding a concentration of 3.70 g/L or 0.23 wt% contaminants. DOP was chosen as the contaminant due to its common use as a plasticizer and the extensive characterization within the other aspects of this work. Testing was completed with the contaminated Novec 649 and comparisons in the performance figures made with those from virgin Novec 649. A significant deterioration in performance was observed in which a noticeable increase in

wall superheat varied with increasing heat flux (Sushil Bhavnani, personal communication, November 12, 2013).

The tank test experimental data runs were completed with microporous heat sinks. These heat sinks were chosen due to their very small surface morphology which would make them most susceptible to changes introduced by the contaminated fluid. It was found that the highly contaminated fluid severely impacted the cooling performance initially provided from clean fluid. It is believed that the deposition of DOP on all surfaces of the small tank, including the printed circuit board and heat sinks, led to interaction with the nucleation sites on the microporous heaters.

In order to demonstrate the ability to successfully remove DOP from the contaminated fluid, 15.35 g of dried activated carbon (Fluval) was added to the two containers shown in Figure 59 and allowed to passively remove DOP for twenty-four hours. Due to space limitations, the amount of carbon used was much less than would be needed for complete removal based on the laboratory scale remediation testing. In real immersion systems, flow through filters could be used or the computing blades could be designed to hold a reasonable amount of material for passive filtration.

The carbon was vacuum dried prior to use and care was taken to prevent moisture absorption before immersion. The activated carbon was allowed to rest inside the tank with contaminated fluid overnight. Fluid samples were collected before and after the run. The limited amount of carbon used still resulted in removal of 6.93 g (7.03 mL) of DOP. The thermal performance after passive filtration was found to be slightly better than it was before the carbon was introduced (Sushil Bhavnani, personal communication, November 12, 2013). Additional carbon or active filtration would have likely resulted in a more

significant change in performance. The pH of the testing fluid was measured at several intervals during testing to ensure that the dielectric properties of the fluid were not altered. No changes were found.

Figure 59. Satchels containing Fluval activated carbon.

Chapter 5

Conclusions and Recommendations

Broad analysis of component material compatibility with three engineered dielectric fluids was conducted. Materials that exhibited greater pliability tended to yield greater amounts of contaminant residues during extraction. These contaminants were linked to polymeric additives such as plasticizers. Generally, more rigid component materials contained fewer plasticizers and showed decreased extraction. It was found that extended material extraction showed increased contaminant elution, beyond the standardized five day testing cycle, but not near the total determined additives of PVC.

No significant effects were seen on the powered structures in the presence of fluid contaminated during accelerated testing, whether near the component material or within the pool of contaminant collection (RBF). Organic contaminants such as plasticizers were shown to be removable via passive introduction of consumer grade activated carbon within a contaminated dielectric fluid. Finally, examination of fluid samples provided from tank testing showed reoccurring contaminants (primarily plasticizers) in both fluid systems, Novec 649 and HFE-7100. Intentionally high levels of contamination did show some changes in thermal properties, most likely due to contaminants at the surface affecting nucleation.

This work has provided a systematic approach to characterizing the interaction of component materials with engineered fluids. It has highlighted the range of possible

materials that could be used in two-phase immersion cooling applications, and that even the same type of materials (e.g., EPDM) can have significantly different types and amounts of leachable components. Therefore a more theoretical approach is needed to replace large scale experimental testing. Additional research to obtain refined solubility parameters would provide a sound thermodynamic basis for selecting materials (both specific material types and additives contained in specific products) would enable more judicious material selection. The results of this work have also shown that real world effects of polymer degradation and decreased pliability on long term component durability should be investigated.

While additional research is needed for detailed design guidelines and lifetime predictions, the results of this work suggest the following design guidelines for passive two-phase immersion cooling in dielectric fluids:

- Soxhlet testing can be used to screen potential materials for significant leaching.
- Novec 649 is preferred over HFE-7100 for its improved thermal and dielectric properties, as well as its lower tendency to extract materials from immersed components.
- Engineered fluid contact with polymeric materials should be minimized.
- Component materials should be chosen that are known to be inert but similarity to the fluid must also be considered. Although polytetrafluoroethylene (PTFE) is highly non-reactive, it exhibits a tendency to swell in the presence of the engineered fluids.

- Polymeric materials coming in contact with the engineered fluids should be rigid and less pliable when possible, or polymeric materials designed to have low leachability should be used.

- Material suppliers should be contacted to obtain low extractable/more chemically inert formulations for transfer tubing, wiring insulation, gaskets, etc.

- Passive or active removal of contamination with high surface area material such as activated carbon should be considered if high levels of fluid contamination are anticipated.

- Due to the potential for acid formation, caution should be used to ensure water is not introduced into Novec 649, however, ambient moisture during fluid handling did not present a concern.

- The engineered fluids can readily absorb into and diffuse through Teflon due to their chemical similarity, however, Teflon wire insulation appears to be acceptable for use. Teflon has the advantage of limited leaching into the engineered fluids.

References

1. Saidur, R., K.Y. Leong, and H.A. Mohammad, *A review on applications and challenges of nanofluids.* Renewable and Sustainable Energy Reviews, 2011. **15**(3): p. 1646-1668.

2. Kandlikar, S.G., *High flux heat removal with microchannels—a roadmap of challenges and opportunities.* Heat Transfer Engineering, 2005. **26**(8): p. 5-14.

3. Wen, D., et al., *Review of nanofluids for heat transfer applications.* Particuology, 2009. **7**(2): p. 141-150.

4. 3M, *3M Novec 649 Engineered Fluid*, in *Product Information.* 2009, Electronics Markets Materials Division

5. 3M, *3M Novec 7100 Engineered Fluid*, in *Product Information.* 2009, Electronics Markets Materials Division.

6. 3M, *3M Fluorinert Electronic Liquid FC-72*, in *Product Information.* 2000, Specialty Materials.

7. Tuma, P.E. *Design considerations relating to non-thermal aspects of passive 2-phase immersion cooling*. in *Semiconductor Thermal Measurement and Management Symposium (SEMI-THERM), 2011 27th Annual IEEE*. 2011.

8. Cray Jr, S.R., *Immersion cooled high density electronic assembly*, 1986, Google Patents.

9. ASTM, *Standard Test Method for Dielectric Breakdown Voltage and Dielectric Strength of Solid Electrical Insulation Materials at Commerical Powere Frequencies*, 2013, ASTM International: West Conshohocken, PA.

10. Leão, F.N. and I.R. Pashby, *A review on the use of environmentally-friendly dielectric fluids in electrical discharge machining.* Journal of Materials Processing Technology, 2004. **149**(1–3): p. 341-346.

11. Barnes, C.M. and P.E. Tuma, *Practical considerations relating to immersion cooling of power electronics in traction systems.* Power Electronics, IEEE Transactions on, 2010. **25**(9): p. 2478-2485.

12. Luque de Castro, M.D. and L.E. García-Ayuso, *Soxhlet extraction of solid materials: an outdated technique with a promising innovative future.* Analytica Chimica Acta, 1998. **369**(1–2): p. 1-10.

13. HallStar, *Monomeric Plasticizers for Flexibile PVC*.

14. Stevens, M.P., *Polymer additives: Part I. Mechanical property modifiers.* Journal of Chemical Education, 1993. **70**(6): p. 444.

15. Stevens, M.P., *Polymer additives: II. Chemical and aesthetic property modifiers.* Journal of Chemical Education, 1993. **70**(7): p. 535.

16. Murphy, J., *Additives for plastics handbook*. 2001: Elsevier.

17. Rahman, M. and C.S. Brazel, *The plasticizer market: an assessment of traditional plasticizers and research trends to meet new challenges.* Progress in Polymer Science, 2004. **29**(12): p. 1223-1248.

18. Wypych, A., *Plasticizers Databook.* 2013: Elsevier.

19. *Phthalate Information Center*. 2013 [cited 2013 December 18]; Available from: http://phthalates.americanchemistry.com/.

20. Shah, B.L. and V.V. Shertukde, *Effect of plasticizers on mechanical, electrical, permanence, and thermal properties of poly(vinyl chloride).* Journal of applied polymer science, 2003. **90**(12): p. 3278-3284.

21. Vahdat, N. and V.D. Sullivan, *Estimation of permeation rate of chemicals through elastometric materials.* Journal of applied polymer science, 2001. **79**(7): p. 1265-1272.

22. Tüzüm Demir, A.P. and S. Ulutan, *Migration of phthalate and non-phthalate plasticizers out of plasticized PVC films into air.* Journal of applied polymer science, 2013. **128**(3): p. 1948-1961.

23. Hedenqvist, M. and U.W. Gedde, *Diffusion of small-molecule penetrants in semicrystalline polymers.* Progress in Polymer Science, 1996. **21**(2): p. 299-333.

24. ASTM, *Standard Test Method for Kauri-Butanol Value of Hydrocarbon Solvents*, 2013, ASTM International: West Conshohocken, PA.

25. Rodriguez, F., *Principles of polymer systems*. Vol. 4. 1996: Taylor & Francis New York.

26. Hildebrand, J.H. and R.L. Scott, *The solubility of nonelectrolytes.* 1955.

27. Hansen, C.M., *Hansen solubility parameters: a user's handbook*. 2007: CRC press.

28. Diky, V., et al., *ThermoData Engine (TDE): Software implementation of the dynamic data evaluation concept. 2. Equations of state on demand and dynamic updates over the web.* Journal of chemical information and modeling, 2007. **47**(4): p. 1713-1725.

29. Frenkel, M., et al., *ThermoData Engine (TDE): software implementation of the dynamic data evaluation concept.* Journal of chemical information and modeling, 2005. **45**(4): p. 816-838.

30. Pfeiffenberger, A., *Dielectric Permittivity Measurements of Electronics Cooling Fluids.* 2013.

31. Ramakrishnan, B., Bhavnani, S. H., Gess, J., Knight, R. W., Harris, D. K., and Johnson, R. W., *Effect of System and Operational Parameters on the Performance of an Immersion-Cooled Multichip Module for High Performance Computing (Accepted)*, in *30th Annual Thermal Measurement, Modeling, and Management Symposium*. 2014, SemiTherm: San Jose, CA.

32. Owen, A., *Fundamentals of UV-visible spectroscopy.* 1996.

33. Settle, F.A., *Handbook of instrumental techniques for analytical chemistry*. 1997: Prentice Hall PTR.

34. Smith, B.C., *Fundamentals of Fourier transform infrared spectroscopy*. 2011: CRC press.

35. Suzuki, H., *Electronic absorption spectra and geometry of organic molecules: An application of molecular orbital theory*. 1967: Elsevier.

36. Griffiths, P. and J.A. De Haseth, *Fourier transform infrared spectrometry*. Vol. 171. 2007: John Wiley & Sons.

37. Feldman, D., *Polymer Barrier Films.* Journal of Polymers and the Environment, 2001. **9**(2): p. 49-55.

38. Singh, R.P., N.S. Tomer, and S.V. Bhadraiah, *Photo-oxidation studies on polyurethane coating: effect of additives on yellowing of polyurethane.* Polymer degradation and stability, 2001. **73**(3): p. 443-446.

39. Barton, A.F.M., *Solubility parameters.* Chemical Reviews, 1975. **75**(6): p. 731-753.

Appendix A – Materials Included in Screening Study

Printed Wiring Boards (PWBs):

1) Megtron6 laminate - no solder mask (from EI)
2) Megtron6 circuit board (scrap Mezz card from EI)
3) KPPE-6053 (from EI)
4) LTCC (9K7 and external metallization) (from UArk)
5) Si + Al-X (from Auburn)
6) Other materials being considered by EI

Packaging materials:

7) Namics U8437-2 underfill
8) Copper
9) Solder alloys (Sn/Pb and SAC 305)
10) Memory module molding compound slug (from ISI)
11) Samsung memory package
12) Micron memory package

Connectors:

13) XCede connector
14) SEARAY connector
15) NeoScale connector
16) Ribbon connector

Optical Modules:

17) Avago

Common materials for fluid containment and transfer:

18) Tygon O-ring
19) Kalrez O-ring
20) Ethylene Propylene Diene Monomer (EPDM) gasket (McMaster and Grainger)
20-1) Ethylene Propylene Diene Monomer (EPDM) sheet
21) Polyvinyl chloride (PVC) tubing
22) Polyethylene (PE) tubing
23) Typical Silicone Pump Tubing
24) Nalgene® 50 Platinum-Cured Silicone Tubing (Phthalate Free)
25) "Natural" Rubber tubing (Red and Black)
26) Latex Rubber Tubing
27) Latex Tubing (White and Black)
28) PFA Tubing (Fluropolymer)
29) Polyurethane Tubing (blue)
29-1) Polyurethane Tubing (clear)
30) Glass tubing
31) Lexan (polycarbonate)
32) Plexiglas (polymethyl methacrylate (PMMA))
33) Quartz

Greases & Sealants:

34) Shin Etsu Thermal Grease G-751
35) TSF-6521C No-Clean Tacky Soldering Flux
36) Vacuum Grease
37) Loctite Polyurethane
38) Cured DURALCO 4538

Wiring with insulation made of:

39) Teflon
40) PVC
41) Nylon
42) Chlorinated Polyethylene
43) Fluorinated Ethylene Propylene (high flexibility)
44) EPDM Rubber Tubing